Ann. Rev. Fluorescence in Spectroscopy: **Submitted: 2008-05-29**

Electronic Energy Transport and Fluorescence Spectroscopy for Structural Insights into Proteins, Regular Protein Aggregates and Lipid Systems

Therese Mikaelsson, Radek Šachl and Lennart B.-Å. Johansson*

Department of Chemistry; Biophysical Chemistry, Umeå University, S-901 87 Umeå, Sweden

ABSTRACT

The present review aims at surveying recent theoretical development and applications of electronic energy transport between chromophoric molecules (*i.e.* donors and acceptors) in various protein and lipid systems. Reversible, partly reversible, as well as irreversible energy transport within pairs of interacting chromophoric molecules are considered. Also energy migration/transfer within ensembles of many donor and acceptor molecules is discussed. An extended Förster theory of interacting pairs is summarised, which brings the analyses of data to the same level of molecular description as in ESR and NMR spectroscopy. Recent applications of energy transfer/migration on protein systems concern their structure, folding, as well as their formation of non-covalent protein polymers. The latter systems are of particular interest in *e.g.* the study of amyloid formation and the molecular functioning of muscles. The energy transfer/migration processes have also been utilised to study the spatial distribution of lipid molecules, which is of interest in the study of biological membranes and their functioning, *e.g.* the presumed formation of so called rafts.

KEY WORDS: Electronic energy transfer/migration, donor-acceptor energy transfer, (partial) donor-donor energy migration, homotransfer, protein polymerisation, lipid membranes, protein folding

LIST OF ABBREVIATIONS

A = acceptor of electronic energy

BD = Brownian dynamics

CTBX = cholera toxin B-subunit

$\chi(t)$ = the time-dependent excitation probability

D = donor of electronic energy

$D(t)$= experimental difference curve created from fluorescence depolarisation data

$\mathbf{D_j}$ = director frame for the j-th donor

DAET = donor-acceptor energy transfer

DDEM = donor-donor energy migration

EFT = extended Förster theory

* Corresponding author, E-mail: lennart.johansson@chem.umu.se, Telephone: +46-(0)90-786 5149, Fax: +46-(0)90-786 7779.

EM = energy migration

(F)RET = (Förster/~~fluorescence~~) resonance energy transfer

$F_D(t)$ = fluorescence relaxation of a donor in absence of acceptors

ϕ_c = the rotational correlation time

$G^s(t)$ = the excitation probability of the initially excited donor

κ = the angular dependence of dipole-dipole coupling

L = the Liouville operator

L = laboratory frame

M= molecule fixed frame

MD = molecular dynamics

MC = Monte Carlo

N = the aggregation number

SLE = stochastic Liouville equation

SME = stochastic master equation

τ_D = the fluorescence lifetime of the donor

PDDEM = partial donor-donor energy migration

pDNA = plasmid DNA

R = the distance between the centres of mass of the donor groups

R = a coordinate system fixed in a protein

R_0 = the Förster radius

r_0 = the fundamental anisotropy

S_j = 2nd rank order parameter

TCSPC = time-correlated single-photon counting

ω = the rate of electronic energy transport

$\Omega = (\alpha, \beta, \gamma)$ = the Eulerian angles of orientation

INTRODUCTION

A diverse of methods based on fluorescence and NMR spectroscopy are frequently applied to study the functioning, structure and dynamics of biomacromolcules, like proteins and nucleic acids, as well as in studies of biological and model membranes. Methods based on X-ray diffraction[1, 2] and NMR spectroscopy[3, 4] are of central importance for the determination of macromolecular structures, and these can often provide three-dimensional structures with atomic resolution. While the former method relies on the preparation of crystals of high quality, the NMR methods may suffer from sufficient spectral resolution for larger molecules. Furthermore NMR is a rather insensitive technique that typically requires

protein concentrations in the mM range, which are often associated with an unwanted protein aggregation. However, intense work has been and still is devoted to the development of complementary methods based on electronic energy transfer and fluorescence spectroscopy. These methods may become important, especially in studies that concern the structure of complex macromolecular assemblies. Most of these applications are based on monitoring the irreversible energy transfer from an excited donor to an acceptor molecule[5-8], while hitherto electronic energy migration between fluorescent molecules of the same kind, so called donor-donor energy migration (DDEM) or homotransfer[9], is used much less frequently.

Distances within macromolecules can be estimated from studies of the electronic energy transfer between extrinsic or intrinsic chromophoric groups localised in macromolecules. The range of distances and the resolution from such experiments is different from that obtained by X-ray and NMR methods. While the X-ray and NMR methods measure short distances, typically representing nearest neighbouring atoms, the fluorescence techniques provide information about longer distances (10 – 100 Å), which are comparable to the size of proteins. The latter range of distances is also representative for intermacromolecular distances within supra-macromolecular structures

NMR spectroscopy[10-13] and X-ray diffraction[14-16] have long been applied to obtain information about structure and dynamics of lipid membrane systems,. For a long time fluorescence quenching has also been extensively applied in various investigations, *e.g.* for the determination of micellar size[17, 18], the size of the building units of cubic liquid crystalline phases[19, 20], as well as to examine the characteristic properties of micro-heterogeneous surfactant and lipid systems[21]. More recently fluorescence experiments have been used to monitor the heterogeneous lipid distributions in giant lipid vesicles[22]. These distributions are sometimes called rafts, and they might be of biological interest.

In quite many applications, donor-acceptor pairs are used to estimate distances in macromolecules and supra-macromolecular structures. This process is here referred to as donor-acceptor energy transfer (DAET). In the literature this process is also named fluorescence resonance energy transfer (FRET). DAET/FRET has been applied in an immense number of studies and publications, and surveys of related papers are found in books describing fluorescence spectroscopy[6, 23], as well as in specialised editions on electronic energy transport[5, 8]. When DAET and extrinsic probes are used to explore macromolecules (*e.g.* proteins or nucleic acids), a major practical difficulty is to achieve specific attachment of one donor and one acceptor group within the *same* macromolecule. This problem is circumvented by using two chemically identical fluorophores in the labelling procedure[24].

Since energy transfer among identical fluorescent groups usually can be considered reversible. Hence, the electronic energy jumps back and forth within a pair, moreover it can migrate among several molecules within an ensemble. For this reason the concept *energy migration* is used to distinguish from the case of irreversible electronic energy transfer. In what follows, the abbreviation DDEM is used for the process of donor-donor energy migration. Although the problem with specific labelling is largely solved, the use of DDEM introduces other methodological questions to solve, which are caused the need of fluorescence depolarisation experiments to monitor the energy migration process. The depolarisation experiments are influenced by the reorienting motions of the fluorophores, as well as the energy migration process, which itself depends on these motions. Therefore, the analysis at a molecular scale becomes rather complex. However, these questions can be sorted out and solved, by adopting an extended Förster theory (EFT)[25, 26], which is presented in this review.

The need to use fluorescent groups, which *irrespective* of their localisation in a macromolecular structure (*e.g.* a protein) exhibit very similar photophysics, limits the applicability of DDEM. Most fluorescent molecules do not fulfil this criterion, whereby the number of useful probes is considerably reduced. Nevertheless, it is possible to make use of the interaction between two chemically identical, but photophysically non-identical donor groups. The energy migration rate within such a DD-pair will influence the photophysics observed, and it is then possible to show how the fluorescence relaxation depends on the rate of energy migration[9, 27]. To distinguish from DDEM and DAET, this case is referred to as partial donor-donor energy migration (PDDEM), because one deals with donor molecules for which the excitation probability is partially reversible. The theoretical treatment of PDDEM is very similar to that of partly reversible DAET[28]. Strictly speaking, PPDEM can occur in any DD-pair, for which each D in the absence of energy migration exhibits non-exponential photophysics[29]. This statement is valid even if the two interacting D-molecules have an identical non-exponential decay[30].

Several biological functions and diseases are connected with proteins which exhibit an inherent ability[31] to form various non-covalent protein polymers. For instance, the α,β,γ-crystallines form rigid three dimensional protein structures, which are of utmost importance for the properties of the human lens[32]. Several diseases are related to non-covalent protein polymers, *e.g.* the formation of amyloids[33, 34] and prions[35, 36]. The cytolytic toxins[37] constitute another interesting class of proteins that form regular proteins aggregates[38, 39], which are thought to create pores in membranes. The X-ray and NMR-methods have the highest potential for exploring such structures at an atomic level. While the challenge of preparing crystal for X-ray should be easier with regularly aggregating proteins, this is in practise not found, where rather mixtures of crystalline structures are obtained. Furthermore the interpretation of NMR data becomes very complicated[40]. This motivates the development of methods

based on fluorescence DAET and DDEM for the study of structures and functioning of non-covalent protein polymers. Recently such a method has been presented[41] and applied to investigate the structure of filamentous actin[42].

A general challenge with fluorescence and electronic energy transfer data concerns the molecular interpretation. A theoretical molecular description involves several parameters, which are usually difficult to unambiguously quantify. In this review, recent theoretical developments are presented together with a new approach to the qualitatively improvement of data analysis. This review also highlights some recent DDEM- and DAET-applications on biomacromolecular systems. In particular, the emphasis is on studies of protein and lipid systems.

THEORETICAL DEVELOPMENT

Applications of electronic energy transfer/migration deal with either pairs or ensembles of interacting chromophores. From a theoretical point of view the former case accounts for the interaction within two particles, while the latter involves a many-particle system with energy transfer/migration among spatially and orientationally distributed molecules. The latter complexity can be handled by combining Monte Carlo (MC) and Brownian dynamics (BD) simulations[41]. Each of these two classes of systems is separately discussed in the following subsections.

Electronic Energy Migration/Transfer within a Pair

Electronic energy transport between two chromophoric molecules can be divided into three separate cases. Each case is dictated by the chemical and photophysical properties of the interacting chromophores. Most often the energy transfer between a donor and an acceptor group is studied, *i.e.* between chemically and photophysically different molecules. This DAET process is schematically illustrated by the reaction

$$D^* + A \longrightarrow D + A^* \qquad (1)$$

The electronic energy is here transferred irreversibly to the acceptor at a rate (ω_{DA}). Thereafter the excited acceptor A* either emits a photon, or relaxes to its electronic ground state via non-radiative routes. For DA pairs an extended Förster theory (EFT) has recently been derived by solving the stochastic master equation (SME) of energy transfer. The SME, which accounts for the reorientational and the spatial dynamics, has been derived from the stochastic Liouville equation (SLE). The solution of the SME provides the following expression of the time-dependent excitation probability $\{\chi(t)\}$ of the donor group[43, 44];

$$\chi(t) = \left\langle exp\left(-\int_0^t \omega(t')dt' \right) \right\rangle F_D(t) \tag{2}$$

In Eq. 2, $F_D(t)$ stands for the fluorescence relaxation of the donor in the absence of an acceptor. The expression within the bracket (<…>) is a stochastic average over the rate of electronic energy transfer between a donor and an acceptor group. The stochastic time-dependent rate of electronic energy transfer is given by;

$$\begin{aligned} &\omega(t) = \Lambda\kappa^2(t) \\ &\Lambda = \frac{3}{2\tau_D}\left(\frac{R_0}{R}\right)^6 \\ &\kappa(t) = \hat{\mu}_A(t)\cdot\hat{\mu}_B(t) - 3(\hat{\mu}_A(t)\cdot\hat{R})(\hat{\mu}_A(t)\cdot\hat{R}) \end{aligned} \tag{3}$$

Here the κ^2-function, Λ, $\hat{R}$ and τ_D denotes the stochastic orientational dependence of the dipole-dipole coupling, a unit vector of the distance vector $\vec{R}\,(=R\cdot\hat{R})$, the coupling strength and the fluorescence lifetime of the donor in absence of an acceptor, respectively. The angles defining the κ^2-function are indicated in Fig. 1. The restricted local reorienting motions of the interacting D and A groups, with respect to the coordinate systems denoted by $\mathbf{D}_A$ and $\mathbf{D}_B$, are described by the transformation angles $\Omega_{M_AD_A}$ and $\Omega_{M_BD_B}$, respectively. The mutual orientation of the director frames $\mathbf{D}_A$ and $\mathbf{D}_B$ relative to a common **R**-frame is described by the angles Ω_{D_iR}, which are referred to as the *configuration angles*. Notice that in the short-time limit, Eq. 2 and the EFT are transferred into the well-known theoretical expression given by Förster´s theory[45], *i.e.* the fluorescence decay of the donor is;

$$\lim_{t\to 0}\chi(t) = exp\left(-\langle\omega\rangle t\right)F_D(t) \tag{4}$$

In Eq. 4 the exponent ($\langle\omega\rangle$) corresponds to the *dynamic* average of the transfer rate between the donor and the acceptor groups. In the numerous applications of Förster's theory, the fluorescence of a donor is monitored in the presence of an acceptor, while both groups are attached to a macromolecule. In the analyses of data it is frequently assumed that the two groups are isotropically oriented, and that the reorienting motions are fast as compared to the rate of energy transfer, *i.e.* in the dynamic limit. In practise these assumptions are usually not fulfilled. In fact, the fluorescence relaxation and the reorienting motions typically occur on the same timescale, *i.e.* in the ns range. Some resulting consequences of these

approximations are illustrated in Fig. 2. Here the D and A groups interact over a fixed distance, which is taken to be $R = 0.8 \cdot R_0$. The donor's lifetime in the absence of A is 10 ns, and both groups undergo rotational motions with a rotational correlation time of ϕ_c = 5 ns. Using the EFT, the time-correlated single-photon counting (TCSPC) data have been created to mimic the corresponding to the D-fluorescence relaxation experiment. According to Eq. 4, the initial decay of the fluorescence relaxation equals the decay expected according to the FT. It is obvious that the FT initially coincides with the EFT (*cf*. Fig. 2), but the two curves gradually diverge over time. Unlike Förster´s theory, the EFT predicts a multi-exponential decay. As a consequence, significant errors in the distance calculations are expected when Förster's theory is used in analyses of experimental data. For isotropic orientation $\langle \kappa^2 \rangle$ = 2/3, the errors can be minimised by determining the initial mono-exponential part of the decay. This means that the decay is fitted to data over the range for which Eq. 4 provides a good statistical fit. Thus, from the value of $\langle \omega \rangle$ obtained and $\langle \omega \rangle = \langle \kappa^2 \rangle \Lambda$, an accurate value of the distance can be calculated.

A second interesting case of energy transport is the reversible migration between two donors that exhibit the same mono-exponential fluorescence decay. This refers to the DDEM process, which is schematically illustrated by the reaction

$$D_A{}^* + D_B \rightleftarrows D_A + D_B{}^* \tag{5}$$

It is obvious that the forward and backward rates of energy migration are equal ($\omega_{AB} = \omega_{BA}$), which implies that the total excitation probability is conserved. Thus, the total excitation probability and the observed fluorescence decay become invariant to the energy migration process. The SME of energy transport for a DD pair can be derived from the stochastic Liouville equation, in a similar manner as was used for DAET. The solution of this SME provides an expression for the time-dependent excitation probability of the primary (p) and secondary (s) excited donor[46]. These excitation probabilities are given by;

$$\begin{aligned}
\chi^{p}(t) &= \frac{1}{2}\left\langle \left[1 + exp\left(-2\int_0^t \omega(t')dt' \right) \right] \right\rangle F_D(t) \equiv \tilde{\chi}^{p}(t) F_D(t) \\
\chi^{s}(t) &= \frac{1}{2}\left\langle \left[1 - exp\left(-2\int_0^t \omega(t')dt' \right) \right] \right\rangle F_D(t) \equiv \tilde{\chi}^{s}(t) F_D(t) \\
\tilde{\chi}^{s}(t) &= 1 - \tilde{\chi}^{p}(t)
\end{aligned} \tag{6}$$

The last equation shows that the excitation due to energy migration is conserved, whereby the total excitation probability, *i.e.* the observable $F_D(t) = \chi^p(t) + \chi^s(t)$, becomes insensitive to the DDEM process. However, information about the DDEM process can be obtained from fluorescence depolarisation experiments. From time-resolved depolarisation experiments the time-resolved fluorescence anisotropy can be constructed[6, 23]. For an ensemble of fluorescent molecules the anisotropy corresponds to an orientational correlation function of second rank according to;

$$r(t) = r_0 \left\langle P_2\left[\hat{\mu}(0)\cdot\hat{\mu}(t)\right]\right\rangle \equiv r_0\rho(t) \tag{7}$$

In Eq. 7 r_0, $\langle.....\rangle$ and P_2 denote the fundamental anisotropy[47], the orientational average over the ensemble and the second Legendre polynomial, respectively. The orientation of the electronic transition dipole moment at the times of excitation ($t = 0$) and emission ($t = t$) are denoted by the unit vectors $\hat{\mu}(0)$ and $\hat{\mu}(t)$. In the following we consider two interacting donor groups (D_A and D_B), which are covalently attached to a macromolecule. Here the macromolecule is assumed to undergo global rotational diffusion like a spherical particle with a characteristic rotational correlation time denoted $\phi_{c,glob}$. Because of energy migration between D_A and D_B, the experimental fluorescence anisotropy $\{r(t)\}$ is composed of the following contributions[26];

$$r(t) = \frac{r(0)}{2}\left[\rho_{AA}(t) + \rho_{BB}(t) + \rho_{AB}(t) + \rho_{BA}(t)\right] exp\left(-t/\phi_{c,glob}\right) \tag{8a}$$

The initial excitation probability of D_A and D_B is equal (= 1/2). The fluorescence anisotropy of each donor in the absence of DDEM is described by $\rho_{ii}(t)$ (i = A or B). The anisotropy contribution due to DDEM from D_i to D_j is given by $\rho_{ij}(t)$. The ρ-terms in Eq. 8a are given by:

$$\rho_{ii}(t) = \left\langle P_2\left[\hat{\mu}_i(0)\cdot\hat{\mu}_i(t)\right]\tilde{\chi}^p(t)\right\rangle \quad i = A,B \tag{8b}$$

$$\rho_{ij}(t) = \left\langle P_2\left[\hat{\mu}_i(0)\cdot\hat{\mu}_j(t)\right]\left(1-\tilde{\chi}^p(t)\right)\right\rangle, \quad i,j = A,B; \left(A \neq B\right) \tag{8c}$$

The third case concerns the energy transport between two chemically identical fluorophores which exhibit different photophysics. This partly reversible process is illustrated by the following reaction:

$$D_A{}^* + D_B \rightleftharpoons D_A + D_B{}^* \tag{9}$$

For this case the time-dependent excitation probabilities of the donors are different, even if for equal rates $\omega_{AB} = \omega_{BA}$. Thus, the PDDEM process represents the intermediate case of DAET and DDEM. An extended Förster theory of PDDEM has also been developed. Starting from the stochastic Liouville equation, it is possible to derive the following stochastic master equation[48]

$$\begin{bmatrix} \dot{\chi}_A(t) \\ \dot{\chi}_B(t) \end{bmatrix} = \begin{bmatrix} -1/\tau_A - \omega(t) & \omega(t) \\ \omega(t) & -1/\tau_B - \omega(t) \end{bmatrix} \begin{bmatrix} \chi_A(t) \\ \chi_B(t) \end{bmatrix} \tag{10}$$

This SME is relevant for two chemically identical donor molecules which exhibit the same absorption and fluorescence spectra, while their fluorescence lifetimes differ. The latter might by due to *e.g.* different chemical environments, or to different exposures of a quencher. For the numerical solution of Eq. 10, it is convenient to adopt the following transformations;

$$\begin{bmatrix} \xi_A(t) = e^{t/\tau_A}\chi_A(t) \\ \xi_B(t) = e^{t/\tau_B}\chi_B(t) \end{bmatrix} \tag{11}$$

whereby the integrated form of Eq. 10 can be written

$$\begin{bmatrix} \xi_A(t) \\ \xi_B(t) \end{bmatrix} = \exp\left\{ \int_0^t 2\omega(s)\mathbf{P}(s)\, ds \right\} \begin{bmatrix} \xi_A(0) \\ \xi_B(0) \end{bmatrix} \tag{12}$$

Here $\mathbf{P}(s)$ stands for the two-dimensional matrix;

$$\mathbf{P}(t) = \begin{bmatrix} -1/2 & (1/2)\exp(\tau_B^{-1} - \tau_A^{-1})t \\ (1/2)\exp(\tau_A^{-1} - \tau_B^{-1})t & -1/2 \end{bmatrix} \tag{13}$$

In studies of PDDEM it is worth noticing that fluorescence lifetime and depolarisation experiments contain information about the excitation probabilities of the donors. Again, we consider two interacting donor groups (A and B), which are attached specifically to *e.g.* a macromolecule. The orientation of the pairs averaged over the ensemble studied is assumed isotropic. For a coupled AB pair, the observed theoretical fluorescence decay of the photophysics $\{s(t)\}$ is given by:

$$s(t) = \tfrac{1}{2} < \chi_A^p(t) + \chi_A^s(t) + \chi_B^p(t) + \chi_B^s(t) > \quad (14)$$

For example, $\chi_A^p(t)$ and $\chi_A^s(t)$ denote the probability that donor A is primarily (p) and excited secondarily (s) by donor B and thereafter emits a photon at the time *t,* respectively. Notice that the observed fluorescence decay is not invariant to the energy migration process as is the case in DDEM. Therefore, a rather complex expression for the fluorescence anisotropy is obtained;

$$r(t) = \frac{r_0 < \rho_{AA}(t)\chi_A^p(t) + \rho_{AB}(t)\chi_B^s(t) + \rho_{BB}(t)\chi_B^p(t) + \rho_{BA}(t)\chi_A^s(t) > exp\left(-t/\Phi_{prot}\right)}{< \chi_A^p(t) + \chi_B^s(t) + \chi_B^p(t) + \chi_A^s(t) >} \quad (15a)$$

where

$$\rho_{ij}(t) = P_2\left[\hat{\mu}_i(0)\cdot\hat{\mu}_j(t)\right] \qquad i,j \in A,B \quad (15b)$$

In the limit of DDEM, *i.e.* for identical fluorescence decays $\{= F_D(t)\}$ of donors A and B, one obtains that[46]

$$\chi_i^p(t) = \tilde{\chi}_i^p(t)F_D(t) = \left\{1 - \tilde{\chi}_i^s(t)\right\}F_D(t) \quad i \in A,B \quad (16)$$

Here the excitation probabilities due to energy migration denoted by $\tilde{\chi}_i(t)$. The following expression of fluorescence anisotropy is then obtained by inserting Eq. 16 into Eq. 15b;

$$r(t) = r_0 < \rho_{AA}(t)\tilde{\chi}_A^p(t) + \rho_{AB}(t)\left\{1 - \tilde{\chi}_A^p(t)\right\} + \rho_{BB}(t)\tilde{\chi}_B^p(t) + \rho_{BA}(t)\left\{1 - \tilde{\chi}_B^p(t)\right\} > exp\left(-t/\Phi_{prot}\right) \quad (17)$$

Thus, by using Eq. 15a it follows that the anisotropy decay is invariant to the photophysics decay as is expected for DDEM.

The different angular transformations needed to evaluate the orientation correlations functions $\rho_{ij}(t)$ are illustrated in Fig. 1. The two correlation functions for which i = j are given by;

$$\rho_{ii}(t) = \sum_{m_i=-2}^{2} \left\langle D_{m_i,0}^{(2)}(\Omega_{M_iD_i}^0) D_{-m_i,0}^{(2)}(\Omega_{M_iD_i}) \right\rangle (-1)^{m_i} \quad (18)$$

while for $i \neq j$ the corresponding functions read:

$$\rho_{ij}(t) = \sum_{q,\,q',m} D^{(2)}_{m,q}(\Omega_{D_iR}) D^{(2)}_{-m,q'}(\Omega_{D_jR}) \left\langle D^{(2)}_{q,0}(\Omega^{0}_{M_iD_i}) D^{(2)}_{q',0}(\Omega_{M_jD_j}) \right\rangle (-1)^{m} \tag{19}$$

The second rank Wigner rotational matrix elements[49], $D^{(2)}_{p,q}(\Omega)$ ($\Omega \equiv \alpha,\beta,\gamma$), depend on the Euler angles $\Omega^{0}_{M_iD_i}$ and $\Omega_{M_iD_i}$ which transform the transition dipole to a fixed and immobilised director frame at the times $t = 0$ and $t = t$. The orientations of the two director frames relative to a common **R**-frame are given by the configuration angles Ω_{D_iR} (*cf.* Fig.1).

In depolarisation experiments the fluorescence intensities $F_{\parallel}$(t) and $F_{\perp}$(t) are collected with the emission polariser set parallel (||) and perpendicular (⊥) relative to the excitation polariser. In terms of contribution from the different correlation functions ($\rho_{ij}(t)$) and excitation probabilities ($\chi^{k}_{m}(t)$, k = p or s and m ∈ A,B) these observables are given by;

$$\begin{aligned} F_{\parallel}(t) &= C\left\{ \sum_{i=A,B} \left\langle \left(1+2\rho_{ii}(t)\right) \chi^{p}_{i}(t) \right\rangle + \sum_{I\neq J=A,B} \left\langle \left(1+2\rho_{ij}(t)\right) \chi^{s}_{i}(t) \right\rangle \right\} \\ F_{\perp}(t) &= C\left\{ \sum_{i=A,B} \left\langle \left(1-\rho_{ii}(t)\right) \chi^{p}_{i}(t) \right\rangle + \sum_{i\neq j=A,B} \left\langle \left(1-\rho_{ij}(t)\right) \chi^{s}_{i}(t) \right\rangle \right\} \end{aligned} \tag{20}$$

DDEM in Regular Polymer Structures

The theoretical description of reversible energy transport among many donors in an ensemble or structure is extremely complex. In the most general case, the rates of energy migration are determined by the reorientation and spatial dynamics, as well as the spatial and orientational distributions of the donors. Unfortunately, there exist no analytical theory that relates the fluorescence depolarisation experiment, or the anisotropy (*r(t)*) to the above mentioned properties. Fortunately, these properties can be taken into account by using BD and MC simulations, as described previously[41]. For describing the local reorientations of the donor bound to a macromolecule, *e.g.* a protein, BD simulations can be implemented by using suitable orienting potentials, usually a Maier-Saupe[50-52] or a cone potential[53, 54]. The parameters of modelling potentials can be adjusted by fitting BD simulations to the experimental orientation correlation functions, which are obtained for the donors in absence of energy migration. To mimic the DDEM among labelled monomers within a regular structure (*cf.* Fig. 3), MC simulations are used. In experiments/simulations this structure is preferably prepared/examined for different mixtures of D-labelled and unlabelled monomers, which then provide independent observations/conditions. In the MC

simulations, the spatial positions of all the donors as well as the neighbours within a certain cut-off distance need to be defined. The BD trajectories are calculated over a long period of time, referred to as T_∞. The total migration rate is calculated from

$$\Omega(t) = \sum_{j=-n}^{n} \omega_{0j}(t) \tag{21}$$

where $\omega_{0j}(t)$ is the rate of energy migration (*cf.* Eq. 3) from the 0:th to the j:th donor. Because the donors undergo reorienting motions on the time scale of migration, κ_{0j}^2 is time-dependent. The coordinates of $\hat{\mu}_j$ with respect to the aggregate fixed frame are given by $\hat{\mu}_j(t) = \vec{A}_{\mu_j}(t) - \vec{O}(T_{XY}, T_Z, \theta, j)$. Here $\vec{A}_{\mu_j}(t)$ denotes the vector directed from the origin of (X_A, Y_A, Z_A) to the point described by $\hat{\mu}_j$ and $\vec{O}(T_{XY}, T_Z, \theta, j)$ describes the position of the centre of mass of the j:th donor (*cf.* Fig. 3).

The first question to answer in the MC simulation is the time (τ_{EM}) *when* an energy migration event takes place. A time interval Δt is chosen, which is smaller than the characteristic time for the variation of $\Omega(t)$ caused by reorienting motions. Hence, $\Omega(t)$ is approximated to be constant within the time interval Δt. Now a random number is generated from a uniform distribution $\eta \in (0,1]$, and τ_{EM} is calculated according to

$$\tau_{EM} = -\frac{1}{\Omega(t)} \ln \eta \tag{22}$$

The obtained value is only accepted if $\eta < \Delta t$, which ensures that the assumption of a constant $\Omega(t)$ is correct. If $\eta > \Delta t$ one steps forward a time unit Δt and calculates $\Omega(t + \Delta t)$. Using this Ω-value, a new random number is generated, and the procedure is repeated until a value of $\eta < \Delta t$ is reached.

The second decision concerns *where* the energy migrates, *i.e.* to which D group among the labelled monomers. From the above calculations one knows the time (T) of the energy migration event. By using BD simulations we can therefore account for the reorienting motions of all donors within the cut-off distance $\vec{A}_{\mu_j}(T)$, which enables calculation of $\kappa_{0j}^2(T)$, $\omega_{0j}(T)$, and $\Omega(T)$. The simulation of the orientational trajectories is performed for all particles in the time window $T \in [0, T_\infty]$ within the cut-off distance, and is only repeated for the new fluorophore when moving along the aggregate. To select the next excited donor, energy migration rates are normalised and sorted in decreasing order according to

$$\left|\omega_{0j}(T)\right| = \frac{\omega_{0j}(T)}{\Omega(T)} \tag{23}$$

Here a random number is generated from a uniform distribution $\eta \in (0,1]$, and the i:th donor is selected for which,

$$\eta \in \left(\sum_{j=1}^{j=i-1} \omega_{0j}(T), \sum_{j=1}^{j=i} \omega_{0j}(T) \right] \tag{24}$$

The calculations above (Eqs. 21-24) account for the local anisotropic motions of the donors groups, *i.e.* energy migration under dynamic conditions. For energy migration in the static limit the scheme also holds, whereas the time-dependence of ω_{0j} and Ω is no longer relevant. The time-dependent fluorescence anisotropy is calculated for times $[T-\tau, T)$ as outlined above until $T \geq T_\infty$. The procedure is repeated many times to form the final ensemble average (= $\langle ... \rangle$):

$$r(t) = r_0 \sum_{j=-n}^{j=n} \left\langle p_j(t) P_2\left(\hat{\mu}_0(0) \cdot \hat{\mu}_j(t)\right) \right\rangle \tag{25}$$

For aggregates effectively being infinitely long, relative to the distance of energy migration, the value of n must be adjusted to probe sufficiently many monomers. When the j:th donor is excited the probability, $p_j(t)$, is set equal to 1, if not it is equal to 0.

To exemplify the influence of aggregate symmetry on the time-resolved fluorescence depolarisation, data have been generated for a configuration (α_{DA}, β_{DA}) and a local order parameter ($=\left\langle D_{00}^{(2)}(\beta_{MD}) \right\rangle \equiv S$) of the donor group, as well as for different labelling efficiencies[41]. Three principal aggregate symmetries were considered namely; the helical, linear and circular one. The influence of dynamics was also examined. The data show (*cf.* Fig. 4) that the energy migration in the static limit is faster in linear and circular aggregates, as compared to the helical geometry. More evident is the large difference between the *r(t)*-decays in the static limit, at low degrees of D-labelling (*f*), and in the presence of reorienting motion of the donor groups. As can be expected this difference decreases with increasing *f*-values, so that the *r(t)*-decays become very similar when approaching 100 % labelling. The DDEM simulation algorithm used also provides information about how far (in terms of the root mean-square displacement) the initial excitation migrates within an aggregate. In units of the average number of Förster radii, one finds that the migration in the linear aggregate is much faster and takes place over a larger distance, as compared to the helical aggregate. This is compatible with the difference in dimensionality and a similar behaviour was previously observed[55]. Because the energy displacement in a ring is directly related to its radius, a

comparison is less straightforward between the circular geometry on one hand, and the helical and linear geometries, on the other.

Electronic Energy Migration/Transfer in Model Membranes

Quite often lipid molecules are labelled with fluorescent groups which are used to probe the membrane in different lateral positions. A realistic scenario is illustrated in Fig. 5, where the fluorescent label is covalently attached to the lipid head-group. If the labels are donor groups, DDEM occurs within and between the bilayer leaflets, *i.e.* as intra- and interlayer migration, respectively. This is also the case if one studies mixtures of donor- and acceptor-labelled lipids. To model the fluorescence relaxation and depolarisation of the donor in DAET and DDEM experiments, one needs to calculate the probability ($=G^{s}(t)$) that the initially excited donor is still excited at a time *t* later. Models for the probabilities of the intra- and interlayer processes have previously been derived[56];

$$ln\,G^{s}_{intra}(t) = -C_2\,\frac{1}{\lambda^{1/3}}\,\Gamma\left(\frac{2}{3}\right)\left(\frac{t}{\tau}\right)^{1/3} \tag{26}$$

$$ln\,G^{s}_{inter}(\mu) = -\frac{C_2}{3\lambda\nu^2}\left(\frac{2}{3}\mu\right)^{1/3}\int_0^{\frac{2\mu}{3}}\left\{1-exp(-s)\right\}s^{-4/3}ds \tag{27}$$

Here C_2 denotes the reduced concentration, which stands for the number of electronically interacting molecules within the area of a circle determined by the Förster radius, R_0. The reduced concentration can be calculated from $C_2 = \pi\rho R_0^2$ with knowledge of the surface acceptor density (ρ). The parameter λ is a number equal to 1 or 2 for DAET and DDEM, respectively. In Eq. 27 $\mu = (3\lambda/2)t\nu^6\tau^{-1}$, $s = \cos^6\theta_r$ and $\nu = R_0 d^{-1}$. Here *d* denotes the distance between the monolayers, which is approximately equal to the thickness of a lipid bilayer (*cf.* Fig. 5). The angle θ_r is between the surface normal and a line connecting the centres of mass of each interacting dipole. For the energy transfer/migration within and between the two-dimensional planes the electronic transition dipoles are approximated to be either isotropic or in-plane oriented[56]. The Eqs. 26 and 27 were derived for *isotropically* oriented transition dipole moments.

The total excitation probability, $G^{s}(t)$, that accounts for both intra- and interlayer energy transfer/migration is given by the joint probability

$$G^{s}(t) = G^{s}_{intra}(t)\prod_{j} G^{s}_{j,inter}(t) \tag{28}$$

In Eq. 28, the multiplication accounts for the general case of energy transfer/migration between several planes of interacting donors/ acceptors. In the case when there is no intralayer energy transport $G^{s}_{intra}(t) = 1$.

For a donor-acceptor system the fluorescence relaxation of the donor is given by

$$F(t) = G^{s}(t) F_{D}(t) \tag{29}$$

To monitor the rate of energy migration among donors one needs to measure the fluorescence depolarisation, which is conveniently expressed by the time-resolved anisotropy, *r(t)*, according to[57]:

$$r(t) = r_0 \left\{ \rho(t) - S^2 \right\} G^{s}(t) + r_0 S^2 \tag{30}$$

Here *S* describes the order of transition dipole *S* with respect to the bilayer normal. The reorientation of the excited donors is described by

$$\rho(t) = \sum a_j \, exp(-t/\phi_j) \tag{31}$$

where ϕ_j are the rotational correlation times which describe the local motions of the donors in the lipid bilayer.

DAET/DDEM in Micelles

When considering electronic energy transfer/migration within vesicles, it is usually not needed to account for the membrane curvature, since the vesicle radii (> 500 Å) are much larger than R_0. However, this approximation is usually not valid for micellar systems, whose radii rarely exceeds 150 Å (see for example reference [58]). In order to account for the micelle curvature, the Eq. (26) above must be slightly modified. When donor and acceptors are distributed on the surface of a sphere (at the core-shell interface of micelles) and all donors occupy equivalent positions one obtains that $G^{s}(t)$) of the donor with respect to DAET[59] is given by;

$$ln\, G^{s}(t) = -2\pi C_A \int_0^{2R_s} r \left\{ 1 - exp\left[-\omega(r) t \right] \right\} dr \tag{32}$$

where C_A is the acceptor surface density, R_s the radius of a sphere, r the distance between the donor and the acceptor and finally $\omega(r)$ stands for the rate of energy transfer of the donor-acceptor pair separated by distance r. This equation can be transferred into a more convenient form[60]

$$ln\,G^s(t) = -C_2\Gamma\left(\frac{2}{3}\right)\left(\frac{t}{\tau_D}\right)^{1/3}\left[1+0.0231\left(\frac{R_0}{R_s}\right)^4\left(\frac{t}{\tau_D}\right)^{2/3} - 7.21\cdot10^{-5}\left(\frac{R_0}{R_s}\right)^{10}\left(\frac{t}{\tau_D}\right)^{5/3}+...\right] \quad (33)$$

For $R_s > R_0$, the time-dependent terms in the bracket ([]) become negligible and the equation transfers into Eq. 26, which accounts for homogenously distributed donors and acceptors in two dimensions (*i.e.* $\lambda = 1$).

From a physical point of view it is reasonable to assume that the donors and the acceptors are spatially distributed in a core-shell interface of thickness Δ (*cf.* Fig. 6), since the core-shell thickness usually cannot be neglected. A more general model that accounts for these circumstances has been derived[60, 61]. The fluorescence decay is then given by

$$F_D(t) = exp\left(\frac{-t}{\tau_D}\right)\int_{V_{mic}} P(r_D)G^s(t,r_D)r_D^{\,2}\,dr_D \quad (34a)$$

$$G^s(t,r_D) = exp\left(\frac{-2\pi}{r_D}\int_{R_e}^{\infty}\{1-exp[-\omega(r)t]\}\left\{\int_{|r_D-r|}^{r_D+r} n_A P(r_A)r_A dr_A\right\}rdr\right) \quad (34b)$$

where V_{mic}, $P(r)$, R_e, and n_A stands for the volume of the micelle, the distribution of donors and acceptors within its interface, the minimal distance between D and A, and for the total number of acceptors within the micelle, respectively (*cf.* Fig. 6). Now imagine that the donors and acceptors are attached between the hydrophobic and hydrophilic block in the place of block junctions. Then, according to Farinha *et al*[62], the distribution of fluorescent probes can be replaced by the distribution of block junctions derived by Helfand and Tagami[63]. The distribution has a shape of inverse hyperbolic cosine function, is less peaked and has broader wings as compared to a Gaussian distribution,

$$P(r) = A\left[cosh\left\{2\left(r-R_s\right)/\Delta\right\}\right]^{-1}. \quad (35)$$

where Δ is assigned to the interface thickness and A is a normalisation constant.

APPLICATIONS OF DAET AND DDEM

Intra- and Intermolecular Distances in Proteins

Few scientists have hitherto used energy migration to determine distances between two chemically identical fluorophores in a protein molecule. Important reasons are the difficulties in obtaining well-defined labelling positions of the interacting chromophores, as well as the complexity in analysing experimental data, which was discussed in the section "Theoretical Development". The energy migration may take place between intrinsic fluorophores, *e.g.* Trp residues[64-66], or between extrinsic probes[67-69] such as *e.g.* BODIPY-derivatives[70-72]. Applications of energy migration has been used to study protein unfolding[67], active sites[65], as well as conformational structures and motions[73, 74]. In these studies more or less qualitative methods were used for analysing the data. Only recently, the extended Förster theory was used for a quantitative analysis of fluorescence depolarisation experiments[26].

Heyn and coworkers[75] have convincingly combined DDEM and DAET experiments to study the dimerisation and inter-chromophore distance in the Cph1 Phytochrome from *Synechocystis*. The chromophore analogue phycoerythrobilin (PEB) was used as the donor group, while either the natural chromophore phycocyanobilin (PCB) or PEB was used as the acceptor in DAET and DDEM studies, respectively. Since each Cph1 monomer has a single binding site for the chromophore, *i.e.* for the PEB or PCB groups, energy migration/transfer occurs within the Cph1 dimer. Time-resolved fluorescence experiments were used to study the PEB/PCB dimers. The average lifetime of PEB was found to decrease linearly with the fraction of occupied PCB sites, which is also expected because the influence of energy transfer increases linearly with the population of DA pairs. For the PEB/PCB dimers, the anisotropy of PEB did not depend on the rate of energy transfer, which is expected if the donor is immobilised on its timescale of fluorescence. The fluorescence depolarisation experiments on PEB/PEB dimers revealed a gradual decrease of the anisotropy decay with increasing concentration of DD pairs, while the lifetime was constant. This clearly shows that DDEM is present within the Cph1 dimers. In the determination of the distance between the PEB-PEB chromophores, the uncertainty of κ^2 was considered. The allowed κ^2-values angles were determined in an elegant manner by combining the anisotropies obtained in the presence of DDEM and knowledge about the twofold symmetry of the dimer.

Recently, Heyn and coworkers[76] have also examined the energy transfer from a single tryptophan to 4-hydroxy-cinnamoyl in a photoactive yellow protein. The aim was to monitor changes of the chromophore structure during the photocycle. For each of the structures corresponding to the two isomerisation states P and I_2, the configuration angles were estimated from the X-ray structure. It was then possible to calculate the κ^2-value and thus predict the rate of energy transfer, which was found to be in excellent agreement with the measured values. The values of the obtained fluorescence anisotropy were compatible with

immobilised chromophores. For the isomerisation of the P to the I_2 structure, the κ^2 value decreased by a factor of 10, whereas the spectral overlap increased by a factor of 2.3. These effects were confirmed from time-resolved fluorescence experiments, which show that the rate of energy transfer is much faster in the P isomer, as compared to the I_2 isomer.

Tryptophan and BODIPY {N-(4,4-difluoro-5,7-dimethyl-4-bora-3a,4a-diaza-sindacene-3-yl)methyl iodoacetamide} is a suitable donor–acceptor pair for intraprotein distance measurements, applicable to the study of protein folding. This is demonstrated in studies of electronic energy transfer between Trp and BODIPY located protein, S6, obtained from *Thermus thermophilus*[77]. Revealing the mechanisms that dictate protein stability is of large relevance for instance to enable design of temperature tolerant enzymes with high enzymatic activity over a large temperature interval. In an effort to identify mechanisms that dictate protein stability the pair Trp–BODIPY has been used in a comparative study of the folding thermodynamics and kinetics of the ribosomal protein S16, which was isolated from a mesophilic and hyperthermophilic bacterium[78].

Non-Covalent Protein Polymers

Proteins may form oligomeric and large aggregates, which constitute regular structures commonly referred to as protein polymers. Using a chemist's terminology, it would be more correct to name the structures non-covalent protein polymers. For instance, transthyretin forms tetramers and mutants of transthyretin form structures, which are associated with the human amyloid disease, *familial amyloidic polyneuropathy*[31, 79]. A common feature of the amyloid diseases is the formation of crystalline non-covalent protein polymers, so called amyloid fibrils. These are, depending on the kind of disease, found as protein deposits in different extra cellular spaces of tissues, or in a few cases as intracellular inclusions. The structure of filamentous actin (F-actin) is another non-covalent polymer, resulting from the spontaneous polymerisation of actin molecules in the presence of salt, and characterized by a fast and a slow growing end where actin subunits add and dissociate in a constant flux balanced by a stable concentration of unpolymerised G-actin. The helically twisted structure of F-actin is of methodological interest in this context since it incorporates special cases of linear and ring-shaped structures[41]. The characteristic parameters of the non-covalent polymer (*cf.* Fig. 3) constitute the translational distance (T_z), the rotation (θ) of each neighbour protein molecule, and the radial distance between the helical axis and the position of the donor (T_{xy}). Recently, the structure of F-actin was studied by performing DDEM experiments and analysing the data by means of Monte Carlo and Brownian dynamics simulations, combined with a fitting procedure, which is based on a genetic algorithm[42]. The method enables prediction of the distribution of a repeating position for the centre of mass of the donor molecule without any *quantitative* preliminary information of the polymer; the only requirement is that the structure is

regular. It was applied to studies of BODIPY-{N-(4,4-difluoro-5,7-dimethyl-4-bora-3a,4a-diaza-*s*-indacene-3-yl)methyl}-labelled filamentous actin. The samples studied were composed of different fractions of labelled actin molecules. The obtained structural parameters T_z and θ were compatible with previously published data[80].

Yeow and Clayton[81] have studied the enumeration of oligomerisation of membrane proteins in living cells by using DDEM and fluorescence depolarisation experiments. In systems exhibiting oligomerisation, the steady-state anisotropy obeys a characteristic feature when plotted as a function of labelling efficiency. The paper also presents a model for interpreting anisotropy data obtained in studies of dilute solutions of oligomers and oligomerisation distributions.

Tubulin is another well-known protein that forms the building unit of microtubules (see *e.g.* reference [82]). Acuna and coworkers[83] have studied the interaction of the anticancer drug Taxol with microtubules.

Micelles

Micelles are built up by a hydrophobic core and shell-forming hydrophilic part and have been studied for decades. The motivations are several, *e.g.* micelles appear useful in applications to environmental questions (removal of organic pollutants), or in pharmaceutical applications as drug releasing units. Although the micellar structure seems simple, micelles may exhibit quite a complex response to physicochemical properties such as, the ionic strength, the solvent polarity, temperature, pH, *etc*[84, 85]. Different techniques have been implemented to elucidate their unique behaviour, ranging from static and dynamic light and neutron scattering, various fluorescence techniques, NMR, AFM, TEM[84, 85], and more recently also electrophoresis[86]. In the following focus will be on the implementation of DAET/DDEM to the study of micellar structures.

Block copolymer micelles. The models of the fluorescence donor decay, which are briefly described in the theoretical section, can be used to obtain information from about the aggregation numbers, (N), the core radius of a micelle and the interfacial thickness. For cases when the higher terms can be neglected in Eq. 33, a similar expression to Eq. 26 has been published[87]. This equation contains the parameter $\xi = 0.339 f_{\mathrm{A}} N \left(R_0 / R_{\mathrm{s}} \right)^2$, which can be determined from experiments. However, neither N nor R_{s} can be determined unless the mole fraction of acceptor (f_{A}) is known[87]. A more extended model[60, 61] accounts also for the finite interfacial thickness {*cf.* Eq. 34-35}. Farinha *et al* have successfully applied this model in studies of a PI-PMMA diblock copolymer dissolved in acetonitrile[62]. For this system the interfacial thickness was estimated to be 9 ± 1 Å. The above model is valid only when donors and

acceptors are distributed within the interface. If this cannot be assumed other models are needed. Jones *et al*[88] have applied such a model for the case of acceptors being solubilised at the interface, while donors are distributed above the surface in a shell. More than thirty years ago Tachiya[17] devolped another model which has been frequently used to determine aggregation numbers. It is then assumed that fluorescent probes residing in a micelle are quenched by quenchers present in the bulk phase. However, the model, although not yet used, should also be applicable to the quenching of donors by acceptors which are incorporated into micelles.

In addition to the above mentioned parameters of micelles, it is also possible to use DAET for determining the critical micelle concentration (cmc), as was shown by Liu *et al*[89]. In this work polystyrene-*block*-poly(2-hydroxyethyl methacrylate) was labelled by either fluorene or pyrene for which a sudden increase of the DAET efficiency was observed upon micelle formation. DAET enables the estimation of cmc, as well as to qualitatively monitor the monomer-micelle equilibrium itself. In such studies two solutions containing micelles are mixed, after being doped with a low fraction of the donor and acceptor labelled monomers, respectively. Upon mixing, the monomers exchange between micelles and the donor intensity decreases over time due to DAET[90].

Towards biological micellar systems. Several research groups have applied DAET to show that the plasmid DNA (pDNA) condenses in confined environments of nanoparticles. These can be of pharmacological interest as potential drug/gene delivery devices[91, 92]. To investigate this idea, Itaka *et al*[91] used pDNA labelled with both fluorescein (donor) and X-rhodamine (acceptor) and followed changes in the donor spectra upon solubilising pDNA in micelles. Since the donor intensity drastically decreased upon binding, it has been suggested that pDNA comprise a more packed (condensed) state in the nano-environment. Itaka *et al* went even further and used this finding to explore the stability of nanoparticles in serum, which could serve as potential gene (DNA) delivery devices. They solubilised pDNA inside a variety of nanoparticles and monitored repeatedly donor spectra in the course of time. While the donor intensity did not change substantially within several hours for pDNA incorporated into poly(ethylene glycol)-poly(L-lysine) micelles, this process was significantly faster for pDNA solubilised in lipoplex particles. The latter is a consequence of the fast degradation of lipoplex particles in serum. Therefore, DAET enables one to observe directly the stability of gene-delivery devices in serum.

Another study that focuses on conformational changes monitored by DAET has been carried out by Kim *et al*[93]. They investigated the conformational switching of a β-amyloid peptide, which is known to be connected with Alzheimer decease. For this purpose, they used the β-amyloid peptide labelled by amine-reactive TMR (donor) and thiol-reactive DABMI, which enabled estimating the DA distances during the

aggregation process. The observed changes in distances with increasing peptide concentration were assigned to monomeric and random coiled amyloid peptides forming micelles, followed by the formation of monomers with β-sheet conformation.

Sarkar *et al*[94] studied the folding of heart cytochrome c using a buffer in absence and presence of urea, and in reverse CTAB micelles. In these experiments a dansyl was covalently attached to the surface of the cytochrome. The dansyl group then acts as a donor to the intrinsic heme group. The structural perturbations observed were compatible with circular dichroism and dynamic light scattering experiments. Recently, Taniguchi *et al*[95] have employed a DAET based method to investigate light-induced structural changes of phoborhodopsin/transducer complex in *n*-dodecyl *β*-D-maltoside micelles. Then the protein complex was labelled at different positions by a DA pair. The absorption spectrum of this pair was not overlapping with that of the protein complex. Hereby it was possible to follow the dynamic change of the protein complex upon excitation. By monitoring the donor intensity, the structural changes decayed at a rate of $1.1 \pm 0.2\ s^{-1}$.

Electronic Energy Transfer in Membranes

Searching for rafts. It has been proposed that the cell membrane may contain liquid-ordered domains, usually called rafts. It is then assumed that these coexist with the liquid-crystalline/liquid-disordered phase of the biomembrane[96]. Since rafts are thought to be involved in various biological functions, such as endo- and exocytosis, cell-cell signalling, and protein sorting[97, 98], any evidence for their existence is of outmost interest. The difference in spatial resolution of the techniques available for exploring membranes is very large. Fluorescence microscopy and AFM reveal domains on the micrometer scale[99], while NMR methods are sensitive to domains on the sub-micrometer scale[100]. Moreover DAET experiments are able to detect heterogeneities as small as few nanometers. Hence, DAET can become an important method in the search for lipid rafts.

To fully utilise the potential of the DAET process, it is important to choose suitable fluorescent probes are needed, which partition differently in crystalline and liquid-ordered phases. If both partners of a DA pair incorporate preferentially in the same phase, the energy transfer rate will increase upon the formation of phase-separated domains. On the other hand, if the probes have different affinity to the phases, energy transfer efficiency decreases as a consequence of donors being separated from acceptors. As a result it is important necessary to also account for the Förster radii, as well as possible dimensions of the presumed lipid rafts. As a rule of thumb, the domain sizes should be comparable to the Förster radius of the DA pair.

To the search for lipid rafts were initiated by Pedersen *et al*[101], who successfully observed domain formation in one model lipid membrane composed of 1,2-dihexadecanoyl-*sn*-glycero-3-phosphocholine, and at temperatures close to the main gel to liquid crystal transition. As a donor-acceptor pair derivatives of phospho-ethanolamine were used, which show different affinity to the coexisting gel/liquid phases. The formation of domains was indicated by the decrease in the donor fluorescence intensity. Later this experimental approach has been extended to the study of more complex systems with an effort to also examine living cells[102, 103].

A slightly different approach based on DAET/DDEM was chosen to prove the intrinsic self-aggregation property of G_{M1} gangliosides in DOPC vesicles[104]. For this purpose, a variety of BODIPY-labelled G_{M1} were synthesised, which could act as DD or DA pairs. The time-resolved fluorescence depolarisation/relaxation data were analysed by means of models, which are very similar to those given by Eqs. 26-31. The model applied is strictly valid for a homogenous distribution of fluorescent probes in membranes. It was found, however, that the recovered reduced concentrations were considerably higher than the values expected for a homogeneous distribution. Therefore the models were modified and synthetic data were generated to mimic various non-uniform distributions of the probes. The reduced concentrations obtained from the reanalyses of these data, were also found significantly higher than the expected ones when using the idealised model. Taken together, this strongly suggests that the G_{M1} lipids show an intrinsic self-aggregation property in lipid bilayers of DOPC.

The determination of raft-sizes from fluorescence decay curves of DAET experiments is a challenging task. Almeida and Loura *et al*[105, 106] have estimated an upper limit of the domain sizes. The follwing modelis assumed:

$$F_{\mathrm{DA}}(t) = x_1 \tilde{G}^{\mathrm{s}}_{\mathrm{intra},1}(t)\tilde{G}^{\mathrm{s}}_{\mathrm{inter},1}(t)F_{\mathrm{D}1}(t) + x_2 \tilde{G}^{\mathrm{s}}_{\mathrm{intra},2}(t)\tilde{G}^{\mathrm{s}}_{\mathrm{inter},2}(t)F_{\mathrm{D}2}(t) \qquad (36)$$

This means that the donor decay in the presence of acceptor $F_{\mathrm{DA}}(t)$ is be expressed as sum of two contributions, the first one originating from the liquid-ordered and the other one from the liquid-disordered phase. In Eq. 36, x_{j} and $F_{\mathrm{Dj}}(t)$ denotes the mole fraction and the fluorescence decay of the donor in the j:th phase, respectively. $\tilde{G}^{\mathrm{s}}_{\mathrm{intra,j}}(t)$ and $\tilde{G}^{\mathrm{s}}_{\mathrm{inter,j}}(t)$ are extended probabilities of $G^{\mathrm{s}}_{\mathrm{intra}}(t)$ and $G^{\mathrm{s}}_{\mathrm{inter}}(t)$, which account for the excluded volume of the donor. One should notice that Eq. 36 only accounts for energy transfer between a donor and an acceptor occupying the same phase. Thus, the domains studied need to be much larger than R_0. The analyses of the donor decays yield that the partition coefficient between both phases of the acceptors. This coefficient can also be obtained in an independent

experiment (*e.g.* from the variation of the lifetime weighted quantum yield or from steady state experiments). From a comparison of the partition coefficient provided by the model, and that obtained independently, the upper limits of domain sizes can be obtained by means of MC simulations[105]. It is found that:

i) The two partition coefficients coincide for domain radius corresponds to at least 15 - 20R_0

ii) The recovered partition coefficient approaches unity if the domain sizes being close to R_0. This is because all acceptors are then distributed randomly in both phases with respect to the donors

iii) For a domain size of ~ 9R_0, the recovered partition coefficient for the acceptor probe is still closer to unity than the input value, which means that the transfer across the interface is not negligible.

Towles *et al*[107] have presented another DAET-approach to the determination of domain sizes. In this work the above presented model was extended. In brief, a constant density of acceptors within a shell around a donor is assumed. The contribution of this shell to the overall decay was estimated and summoned up over the whole space. An analytical expression for the donor decay was derived for heterogeneously distributed acceptors. Numerical calculations were used to estimate the average probability of finding a domain at a distance from the point where the initially excited donor is located. The donor decay is expressed as

$$F_{\mathrm{DA}}(t) = F_{\mathrm{D}}(t)\prod_{\mathrm{j}=1}^{\infty}\frac{\left[\tilde{G}^{\mathrm{s}}_{\mathrm{intra}}(t)\tilde{G}^{\mathrm{s}}_{\mathrm{inter}}(t)\right]_{R_{\mathrm{ex}}=\eta_{\mathrm{j}}}}{\left[\tilde{G}^{\mathrm{s}}_{\mathrm{intra}}(t)\tilde{G}^{\mathrm{s}}_{\mathrm{inter}}(t)\right]_{R_{\mathrm{ex}}=\eta_{\mathrm{j}+1}}} \qquad (37)$$

where R_{ex} is the radius of the excluded zone (shell), η is the thickness of the shell and the survival probability $\tilde{G}^{\mathrm{s}}_{\mathrm{j}}(t)$ (J = intra, inter) depends on the distribution of acceptors surrounding the donors. From a comparison of the analytical model with MC simulations it was concluded that the model predicts domains sizes within an accuracy of ~ 20 %, for domain sizes < 4R_0. In addition to the above mentioned models, another one there also exists that enables an estimation of domain sizes from fluorescence steady-state experiments. Using this model heterogeneities both in binary and ternary systems have been reported[108].

Interaction membrane-peptide/-protein. Lipids play a crucial role in protein/peptide assembling behaviour. Interestingly, some helical peptides that by themselves do not assemble, actually form peptide-peptide assemblies in the presence of lipids bilayer[109]. Sparr *et al*[110] have studied self-association of transmembrane α-helices in model membranes by means of DAET and the formation of pyrene excimers. Either the C or N terminus of the peptide was labelled by pyrene. The efficiency of excimer formation

was compared for C-C, C-N and N-N pyrene-labelled peptides. Supporting information has been obtained by DAET between the intrinsic tryptophan group and pyrene labelled helices. The self-association of α-helices that did not contain any specific recognition motive occurred almost exclusively between antiparallel helices. Relatively high peptide/lipid ratios (at least 1/25) were needed to obtain association in DOPC vesicles. Self-assembly was promoted by an increase, as well as a decrease of the bilayer thickness because of the increased mismatch[111] between the bilayer thickness and the hydrophobic length of the peptide. It was therefore concluded that the lipids influence the association of α-helices.

The specific interactions between rhodopsine and the G-protein in phospholipid vesicles have been studied by DAET[112]. For this purpose, these molecules were labelled with coumarin or pyrene, which form an efficient DA pair. Since the G-protein can bind to the membrane by non-specific interactions, additional experiments were carried for estimating this fraction. In the first experiment non-hydrolysable analogues were added of GTP, which promote dissociation of the rhodopsine-G-protein complex. In further experiments excess of unlabeled G-protein was added, which competes for the binding sites in rhodopsine. It was possible to observe specific binding of the G-protein, even in the presence of non-specific interactions with a membrane.

In a complex DAET study Loura *et al* have studied the interaction of the K6W peptide with lipid bilayers composed of dipalmitoyl-phosphatidylcholine and dipalmitoyl-phosphatidylserine[113]. These model membranes were examined at two temperatures (45 or 60 ˚C) and for different peptide concentrations. The DA-pair used was DPH-labelled phosphocholine (donor) and NBD-labelled phosphocholine (acceptor). The donor group is preferably located in the hydrophobic part, while the acceptor group is likely localised in the interface region of the membrane. Therefore energy transfer occurs between a plane of randomly spaced donors and two more planes containing the acceptors located in the opposite interfaces. A model accounting for this case was successfully applied only in the presence of the peptide at the lower temperatures. The data obtained for the higher temperature are compatible with heterogeneous lipid bilayers (containing domains). This was concluded from the donor decay in the presence of acceptor, which could be described by asssuming two infinitively separated phases (see above). Although addition of peptide did not cause any substantial perturbations to the heterogeneous membrane at the lower temperature, the DAET efficiency changed drastically for the previously homogenous membrane. Interestingly, no improvement in describing the donor decay was obtained by a model which accounts for the two-phase separation. Because the peptide is positively charged and the lipid bilayer is negative the formation of multi-bilayers was suggested, where stacking is promoted by the peptides. The data were also analysed with a model that describes DAEt between two or more bilayers from which a repeat distance of 57 Å was obtained.

A very similar approach was used to prove the self-aggregation property of G_{M1} (see above) can also be applied in the study of peptide/protein aggregation in membranes. Several years ago this was demonstrated by Bogen *et al*[114] in studies of the WALP16 peptide labelled with rhodamine 101. The obtained reduced concentration for the transmembrane peptide WALP16 was about 10 times higher than that expected for randomly distributed peptides.

Pore formation. The action of some antibacterial molecules is ascribed to their presumed ability to form pores in the membrane. Although several investigators have addressed this question[115, 116] a minority of them make use of the DAET/DDEM techniques. A possible explanation is the lack of fluorescent compounds that would preferentially reside inside pores. Rather, other methods have been used, such as the measurements of leakage of fluorescent probes from the inside of vesicles[116], or fluorescence microscopy[117]. A real challenge would be to estimate the pore size by means of the DDEM methods.

Viero *et al*[118] have published an interesting DAET study on the pore formation. They observed the oligomerisation of two different proteins HlgA/HlgB in a model membrane. Site specific mutagenesis was used to replace certain residues of HlgA and HlgB by cysteine. These Cys groups were labelled with ALEXA-488 (donor) and ALEXA-546 (acceptor). The mutated residues were deliberately selected on the right or left site of the protein surfaces. The reason of the choice was a proposal that the wall of the pore is build up by rings consisting of alternating HlgA/HlgB proteins. From an analysis of the energy transfer efficiency for all possible DA pairs (such as $HlgA_{right}/HlgB_{right}$, $HlgA_{left}/HlgB_{right}$ *etc*.) it was shown that heterogeneous interfaces HlgA/HlgB or HlgB/HlgA have a much higher affinity than corresponding HlgA/HlgA, HlgB/HlgB pairs. In another study of pore formation Silva *et al*[119] labelled an amino group of nystatin polyene molecule by NBD. The intention was to prove the ability of the nystatin polyene molecule to aggregate and form pores in lipid membranes by means of DDEM. Surprisingly, they could not confirm the previous results obtained by O'Neill *et al*[120], who observed pore formation by photo-bleaching measurements. The authors have suggested[119] that the function of the NBD-labelled amino group is crucial for the action of nystatin.

Membrane-DNA interactions. There are surprisingly few fluorescence spectroscopic studies of lipid-DNA interactions. However, such methods have been applied to examine the encapsulation efficiency into lipoplex particles (*cf.* the above section about micelles and a paper by Madeira *et al*[121] for further references). Madeira *et al*[121] were among the first to apply DAET/DDEM in quantitative studies. DNA/lipid complexes were examined by DAET by using DNA, labelled by either BOBO-1 (donor) or ethidium bromide (acceptor). The charged membrane was doped with either DPH-PC (donor) or

BODIPY-PC (acceptor). It was confirmed that the DNA molecules intercalate between membranes and orient with their long axis parallel to the bilayer surface. In the theoretical modelling it was therefore assumed that the donors and acceptors are randomly distributed in different parallel planes. Since there was an indispensable fraction of unbound DNA, the authors modified the theoretical model, depending on whether the DNA served as a donor or acceptor. From the analyses of the fluorescence decays, the distance between membrane-bound DNA and the donors/acceptors which were attached to the PC chain was obtained, as well as the encapsulation efficiencies.

Approaching studies of the living cell. Up to now this review has dealt with model membranes, which are more or less relevant for mimicking the properties of biological membranes. Nevertheless this approach is useful, especially for testing complex models aimed for quantitative studies. In studies of really complex systems, such as living cells, it is usually very difficult to determine absolute values of energy transfer efficiencies, and a more qualitative approach is wanted. For instance, the aim might be to study the formation of various associates (like protein dimers, lipid domains *etc*.) in living cells. It is then necessary to find out whether the donors and acceptors involved in the formation of studied aggregates are randomly distributed in the membrane, or whether they form aggregates and/or partition into the domain structure. For exploring this, the energy transfer efficiency is usually monitored as a function of the acceptor surface density and the molar donor/acceptor ratio. For donors and acceptors forming aggregates, the DAET efficiency depends on the donor/acceptor ratio, and it is independent of the surface density of acceptors. On the other hand, for randomly distributed probes, the DAET efficiency increases with increasing surface density of the acceptors. This methodology has been applied, for example by Herrick-Davis *et al*[122], who studied the formation of homo-dimers of serotonin-$5HT_{2C}$ in the membrane of living cells. In addition to DAET, bioluminescence and energy transfer was used in studies which do not require an external excitation by for instance a laser.

The above outlined concept has also been frequently used to prove the presumed existence of rafts in living cells. However, this proposal is still controversial, as is evident from the review by Silvius *et al* [123]. For example, Kenworthy *et al*[124] monitored energy transfer between the donor- and acceptor-labelled cholera toxin B-subunit (CTBX), between donor- and acceptor-labelled GPI-anchored proteins and CTBX, as well as between CTBX and GPI-anchored proteins in living cells. It was found that the DAET efficiency correlates with the acceptor surface density, and it approaches zero at low surface densities. This is indeed consistent with randomly distributed probes within cell membranes, and consequently with no or a very low formation of rafts. Sharma *et al*[125] have used GPI-anchored fluorescent proteins (GFP or mYFP) and the GPI-anchored folate receptor to monitor the raft formation by means of both DDEM and DAET. The analysis of the depolarisation data suggests that the fractions of

rafts are 20 - 40 %. Their size is estimated to be less than 5 nm in diameter and they comprise 4 - 5 GPI molecules. Notice however, that the DAET studies by Kenworthy *et al*[124] did not reveal any formation of rafts. A possible explanation might be that the DDEM method in the present case is more sensitive to small heterogeneities, which consist of only *ca*. 4 - 5 molecules. Sengupta *et al*[126] have recently investigated inhomogeneities in plasma membranes by labelling lipids with carbocyanine derivatives of different acyl chain length. These studies provide consistent results from DAET as well as DDEM experiments, which are compatible with the existence of nanometer sized domains.

Acknowledgements

This work was financially supported by the Swedish Research Council. We are grateful to Mr. Oleg Opanasyuk for preparing the figures 3 and 6.

References

[1] R.E. Dickerson, X-ray analysis and protein structure, Academic Press, New York, 1964.
[2] T.L. Blundell, L.N. Johnson, Protein Crystallography, Academic Press, London, 1976.
[3] G.M. Clore, A.M. Gronenborn, Topics in Molecular and Structural Biology, The Macmillan Press Ltd, London, 1993.
[4] K. Wütrich, NMR of Proteins and Nucleic Acids, Wiley, New York, 1986.
[5] B.W. Van der Meer, G. Coker III , S.-Y.S. Chen, Resonance Energy Transfer: Theory and Data, VCH Publishers, Inc., 1994.
[6] B. Valeur, Molecular Fluorescence. Principles and Applications., Wiley-VCH, 2002.
[7] J.R. Lakowicz, Principles of Fluorescence Spectroscopy, 2nd ed., Kluwer Academic/Plenum Publishers, New York, 1999.
[8] N.L. Vekshin, Energy Transfer in Macromolecules, Spie Press, 1997.
[9] S. Kalinin, L.B.-Å. Johansson, Utility and Considerations of Donor-Donor Energy Migration as a Fluorescence Method for Exploring Protein Structure-Function, J. Fluorescence 14 (2004) 681-691.
[10] J.H. Davis, Deuterium nuclear magnetic resonance and relaxation in partially ordered systems., Adv. Magn. Reson. 13 (1989) 195-223.
[11] G. Lindblom, G. Orädd, NMR studies of translational diffusion in lyotropic liquid crystals and lipid membranes., Progr. Nucl. Magn. Reson. Spectrosc. 26 (1994) 483-516.
[12] J.H. Davis, M. Auger, Static and magic angle spinning NMR of membrane peptides and proteins., Prog. NMR Spectrosc. 35 (1999) 1-84.
[13] G. Orädd, G. Lindblom, Lateral diffusion studied by pulsed field gradient NMR oriented lipid membranes., Magn. Reson. Chem. 42 (2004) 123-131.
[14] F. Österberg, L. Rilfors, Å. Wieslander, G. Lindblom, S.M. Gruner, Lipid extracts from membranes of Acholeplasma laidlawii. A grown with different fatty acids have a nearly constant spontaneous curvature., Biochim. Biophys. Acta 1257 (1989) 18-24.
[15] M.W. Tate, E.F. Eikenberry, D.C. Turner, E. Shyamsunder, S.M. Gruner, Nonbilayer phases of membrane lipids., Chem. Phys. Lipids 57 (1991) 147-164.
[16] G.C. Shearman, O. Ces, R.H. Templer, J.M. Seddon, Inverse lyotropic phases of lipids and membrane curvature, J. Phys.: Condens. Matter 18 (2006) 1105–1124.
[17] M. Tachiya, Application of a Generating Function to Reaction Kinetics in Micelles. Kinetics of Quenching of Lumuniscence Probes in Micelles, Chem. Phys. Letters 33 (1975) 289-292.
[18] M. Almgren, J.-E. Löfroth, Effects of polydispersity on fluorescence quenching in micelles, J. Chem. Phys. 76 (1982) 2734-2743.

[19] O. Söderman, L.B.-Å. Johansson, The Cubic Phase (I1) in the Dodecyltrimethylammonium Chloride/Water System. A Fluorescence Quenching Study, J. Phys. Chem. 91 (1987) 5275-5278.
[20] O. Söderman, L.B.-Å. Johansson, Aggregate Size and Surfactant/Hydrocarbon Diffusion in the Cubic Phase of Sodium Octanoate/Hydrocarbon/Water., J. Coll. Interface Sci. 179 (1996) 570.
[21] M. Almgren, Diffusion-Iinfluenced Deactivation Processes in the Study of Surfactant Aggregates, Adv. Colloid and Interface Sci. 41 (1992) 9-32.
[22] L.A. Bagatolli, Direct observation of lipid domains in free standing bilayers:
from simple to complex lipid mixtures, Chem. Phys. Lipids 122 (2003) 137-145.
[23] J.R. Lakowicz, Principles of Fluorescence Spectroscopy, 3rd ed., Springer, Singapore, 2006.
[24] J. Karolin, M. Fa, M. Wilczynska, T. Ny, L.B.-Å. Johansson, Donor-Donor Energy Migration (DDEM) for Determining Intramolecular Distances in Proteins: I. Application of a Model to the Latent Plasminogen Activator Inhibitor-1 (PAI-1), Biophys. J. 74 (1998) 11-21.
[25] L.B.-Å. Johansson, F. Bergström, P. Edman, I.V. Grechishnikova, J.G. Molotkovsky, Electronic Energy Migration and Molecular Rotation within Bichromophoric Macromolecules. Part 1. Test of a Model using bis(9-anthrylmethylphosphonate) bisteroid, J. Chem. Soc., Faraday Trans. 92 (1996) 1563-1567.
[26] M. Isaksson, P. Hägglöf, P. Håkansson, T. Ny, L.B.-Å. Johansson, Extended Förster Theory for Determining Intraprotein Distances: 2. An Accurate Analysis of Fluorescence Depolarisation Experiments, Phys. Chem. Chem .Phys. 9 (2007) 3914-3922.
[27] S.V. Kalinin, J.G. Molotkovsky, L.B.-Å. Johansson, Partial Donor-Donor Energy Migration (PDDEM) as a Fluorescence Spectroscopic Tool of Measuring Distances in Biomacromolecules, Spectrochim. Acta Part A 58 (2002) 1087-1097.
[28] P. Woolley, K.G. Steinhauser, B. Epe, Forster-Type Energy-Transfer - Simultaneous Forward and Reverse Transfer between Unlike Fluorophores, Biophysical Chemistry 26 (1987) 367-374.
[29] M. Isaksson, S. Kalinin, S. Lobov, S. Wang, T. Ny, L.B.-Å. Johansson, Distance Measurements in Proteins by Fluorescence Using Partial Donor-Donor Energy Migration (PDDEM), Phys. Chem. Chem. Phys. 6 (2004) 3001-3008.
[30] S. Kalinin, L.B.-Å. Johansson, Energy Migration and Transfer Rates are Invariant to Modelling the Fluorescence Relaxation by Discrete and Continuous Distributions of Lifetimes, J. Phys. Chem. B 108 (2004) 3092-3097.
[31] C.M. Dobson, Protein folding and misfolding, Nature 426 (2003) 884-890.
[32] C.A. Paterson, N.A. Delamere, The lens, 9th ed., Mosby-Year Book, St. Louis, 1992.
[33] M. Malisauskas, V. Zamotin, J. Jass, W. Noppe, C.M. Dobson, L.A. Morozova-Roche, Amyloid protofilaments from the calcium-binding protein equine lysozyme: Formation of ring and linear structures depends on pH and metal ion concentration, J. Molec. Biol. 330 (2003) 879-890.
[34] M. Malisauskas, J. Ostman, A. Darinskas, V. Zamotin, E. Liutkevicius, E. Lundgren, L.A. Morozova-Roche, Does the cytotoxic effect of transient amyloid oligomers from common equine lysozyme in vitro imply innate amyloid toxicity?, J. Biol. Chem. 280 (2005) 6269-6275.
[35] A. Aguzzi, M. Polymenidou, Mammalian prion biology: One century of evolving concepts, Cell 116 (2004) 313-327.
[36] F. Houston, W. Goldmann, A. Chong, M. Jeffrey, L. Gonzalez, J. Foster, D. Parnham, N. Hunter, Prion diseases: BSE in sheep bred for resistance to infection, Nature 423 (2003) 498-498.
[37] S.N. Wai, M. Westermark, J. Oscarsson, J. Jass, E. Maier, R. Benz, B.E. Uhlin, Characterisation of Dominantly Negative Mutant ClyA Cytotoxin Proteins in *Echerichia coli*, J, Bacteriol. 185 (2003) 5491-5499.
[38] P. Stanley, V. Koronakis, C. Hughes, Acylation of *Escherichia coli* hemolysin: a unique protein lipidation mechanism underlaying toxin function, Microbiol. Mol. Biol. Rev. 62 (1998) 309-333.
[39] L. Abrami, M. Fivaz, F.G. van der Goot, Adventures of a pore-forming toxin at the target cell surface, Trends Microbiol. 8 (2000) 168-172.
[40] A. Olofsson, A.E. Sauer-Eriksson, A. Öhman, The Solvent Protection of Alzheimer Amyloid-b-(1–42) Fibrils as Determined by Solution NMR Spectroscopy, J. Biol. Chem. 281 (2006) 477-483.

[41] D. Marushchak, L.B.-Å. Johansson, On the Quantitative Treatment of Donor-Donor Energy Migration in regularly Aggregated proteins, J. Fluoresc. 15 (2005) 797-804.
[42] D. Marushchak, S. Grenklo, T. Johansson, R. Karlsson, L.B.-Å. Johansson, Fluorescence Depolarisation Studies of Filamentous Actin Analysed with a Genetic Algorithm, Biophys. J. 93 (2007) 3291–3299.
[43] P.-O. Westlund, H. Wennerström, Electronic energy transfer in liquids. The effect of molecular dynamics., J. Chem. Phys. 99 (1993) 6583-6589.
[44] M. Isaksson, N. Norlin, P.-O. Westlund, L.B.-Å. Johansson, On the Quantitative Molecular Analysis of Electronic Energy Transfer within Donor-Acceptor Pairs, Phys. Chem. Chem .Phys. 9 (2007) 1941–1951.
[45] T. Förster, Zwischenmolekulare Energiewanderung und Fluorescenz, Ann. Phys. 2 (1948) 55-75.
[46] L.B.-Å. Johansson, P. Edman, P.-O. Westlund, Energy migration and rotational motion within bichromophoric molecules. II. A derivation of the fluorescence anisotropy, J. Chem. Phys. 105 (1996) 10896-10904.
[47] A. Jablonski, Influence of torosional vibrations of luminescent molecules on the fundamental polarisation of photoluminiscence of solutions, Acta Phys. Polon. 10 (1950) 33-36.
[48] N. Norlin, P. Håkansson, P.-O. Westlund, L.B.-Å. Johansson, Extended Förster Theory of Partial Donor-Donor Energy Migration (PPDEM): The κ^2-Dynamics and Fluorophore Reorientation. , PCCP, submitted (2008).
[49] D.M. Brink, G.R. Satchler, Angular Momentum, Clarendon Press, Oxford, 1993.
[50] M. Doi, J. Polymer. Sci. Poly. Phys. Ed. 19 (1981) 229.
[51] W. Maier, A. Saupe, Z. Naturforsch. A 14 (1959) 882-889.
[52] H.C. Öttinger, Stochastic processes in polymeric fluids, Springer, Berlin, Heidelberg, New York, 1996.
[53] I. Fedchenia, P.-O. Westlund, U. Cegrell, Brownian dynamic simulation of restricted molecular diffusion the symmetric and deformed cone model., Molecular Sim. 11 (1993) 373.
[54] W.H. Press, S.A. Teukolsky, B.P. Flannery, Numerical Recipes in C, Cambridge, England, 1992.
[55] L.B.-Å. Johansson, S. Engström, M. Lindberg, Electronic energy transfer in anisotropic systems. III. Monte Carlo simulations of energy migration in membranes, J. Chem. Phys. 96 (1992) 3844-3856.
[56] J. Baumann, M.D. Fayer, Excitation transfer in disordered two-dimensional and anisotropic three dimensional systems: Effects of spatial geometry on the time-resolved observables, J. Chem. Phys. 85 (1986) 4087-4108.
[57] B. Medhage, E. Mukhtar, B. Kalman, L.B.-Å. Johansson, J.G. Molotkovsky, Electronic energy transfer in anisotropic systems. 5. Rhodamine-lipid derivatives in model membranes, J. Chem. Soc., Faraday Trans. 88 (1992) 2845-2851.
[58] R. Xu, M.A. Winnik, G. Riess, B. Chu, M.D. Croucher, Micellization of Polystyrene-Poly(ethylene oxide) Block Copolymers in Water. 5. A Test of the Star and Mean-Field Models., Macromolecules 25 (1992) 644-652.
[59] P. Levitz, J.M. Drake, J. Klafter, Critical evaluation of the application of direct energy transfer in probing the morphology of porous solids., J. Chem. Phys. 89 (1988) 5224-5236.
[60] A. Yekta, M.A. Winnik, J.P.S. Farinha, J.M.G. Martinho, Dipole-Dipole Electronic Energy Transfer. Fluorescence Decay Functions for Arbitrary Distributions of Donors and Acceptors. II. Systems with Spherical Symmetry., J. Phys. Chem. A 101 (1997) 1787-1792.
[61] J.P.S. Farinha, J.M.G. Martinho, S. Kawaguchi, A. Yekta, M.A. Winnik, Latex Film Formation Probed by Nonradiative Energy Transfer: Effect of Grafted and Free Poly(ethylene oxide) on a Poly(n-butyl methacrylate) Latex., J. Phys. Chem. 100 (1996) 12552-12558.
[62] J.P.S. Farinha, K. Schillén, M.A. Winnik, Interfaces in Self-Assembling Diblock Copolymer Systems: Characterization of Poly(isoprene-b-methyl methacrylate) Micelles in Acetonitrile, J. Phys. Chem. B 103 (1999) 2487-2495.
[63] E. Helfand, Y. Tagami, Theory of the Interface between Immiscible Polymers. II., J. Chem. Phys. 56 (1972) 3592-3601.

[64] A.H.C. de Oliveira, J.R. Giglo, S.H. Andrião-Escarso, R.J. Ward, The Effect of Resonance Energy Homotransfer on the Intrinsic Tryptophan Fluorescence Emission of the Bothopstoxin-I Dimer, Biochem. Biophys. Res. Comm. 284 (2001) 1011-1015.
[65] M. Kyoung, S.Y. Kim, H.-Y. Seok, I.-S. Park, M. Lee, Probing the Caspase-3 Active Site by Fluorescence Lifetime Measurements, Biochem. Biophys. Acta 1598 (2002) 74-79.
[66] P.D.J. Moens, M.K. Helms, D.M. Jameson, Detection of Tryptophan to Tryptophan Energy Transfer in Proteins, The Protein Journal 23 (2004) 79-83.
[67] X. Duan, Z. Zhao, J. Ye, H. Ma, A. Xia, G. Yang, C.-C. Wang, Donor-Donor Energy-Migration Measurements of Dimeric DsbC Labeled at its N-Terminal Amines with Fluorescent Probes: A Study of Protein Unfolding, Angew. Chemie Internat.Ed. 43 (2004) 4216-4219.
[68] M. Fa, F. Bergström, J. Karolin, L.B.-Å. Johansson, T. Ny, Conformational studies of plasminogen activator inhibitor type 1 by fluorescence spectroscopy: Analysis of the reactive centre of inhibitory-, substrate- and reactive centre cleaved forms, Eur. J. Biochem. 267 (2000) 3729-3734.
[69] P. Zou, K. Surendhran, H.S. Mchaourab, , Distance Measurements by Flourescence Energy Homotransfer: Evaluation in T4 Lysozyme and Correlation with Dipolar Coupling between Spin Labels, Biophys. J: Biophys. Letters 92 (2007) L27-L29.
[70] F. Bergström, I. Mikhalyov, P. Hägglöf, R. Wortmann, T. Ny, L.B.-Å. Johansson, Dimers of Dipyrrometheneboron Difluoride (BODIPY) with Light Spectroscopic Applications in Chemistry and Biology, J. Am. Chem. Soc. 124 (2002) 196-204.
[71] J. Karolin, L.B.-Å. Johansson, L. Strandberg, T. Ny, Fluorescence and Absorption Spectroscopic Properties of Dipyrrometheneboron Difluoride (BODIPY) Derivatives in Liquids, Lipid Membranes, and Proteins, J. Am. Chem. Soc. 116 (1994) 7801-7806.
[72] D. Marushchak, S. Kalinin, I. Mikhalyov, N. Gretskaya, L.B.-Å. Johansson, Pyrromethene dyes (BODIPY) can form ground state homo and hetero dimers: Photophysics and spectral properties, Spectrochim. Acta, A 65 (2006) 113–122.
[73] M. Wilczynska, M. Fa, J. Karolin, P.-I. Ohlsson, L.B.-Å. Johansson, T. Ny, Structural insights into serpin-protease complexes reveal the inhibitory mechanism of serpins, Nat. Struct. Biol. 4 (1997) 354-356.
[74] M. Wilczynska, S. Lobov, P.-I. Ohlsson, T. Ny, A redox-sensitive loop regulates plasminogen activator inhibitor type-2 (PAI-2) polymerization., EMBO J. 22 (2003) 1753-1761.
[75] H. Otto, T. Lamparter, B. Borucki, J. Hughes, M.P. Heyn, Dimerization and Inter-Chromophore Distance of Cph1 Phytochrome from Synechocystis, as Monitored by Fluorescence Homo and Hetero Energy Transfer, Biochemistry 42 (2003) 5885-5895.
[76] H. Otto, D. Hoersch, T. Meyer, M. Cusanovich, M.P. Heyne, Time-Resolved Single Tryptophan Fluorescence in Photoactive Yellow Protein Monitors Changes in the Chromophore Structure during the Photocycle via Energy Transfer, Biochemistry 44 (2005) 16804-16816.
[77] M. Olofsson, S. Kalinin, M. Oliveberg, L.B.-Å. Johansson, Tryptophan – BODIPY: A Versatile Donor-Acceptor Pair for Probing Generic Changes of Intraprotein Distances, Phys. Chem. Chem. Phys. 8 (2006) 3130 - 3140.
[78] M. Wallgren, J. Jörgen Åden, O. Pylypenko, T. Mikaelsson, L.B.-Å. Johansson, A. Rak, M. Wolf-Watz, Extreme temperature tolerance of a hyperthermophilic protein coupled to residual structure in the unfolded state, J. Mol. Biol. In press (2008).
[79] J.-C. Rochet, P.T. Lansbury, Jr, Amyloid fibrillogenesis: themes and variations, Curr. Opin. Struct. Biol. 10 (2000) 60-68.
[80] E. Egelman, The structure of F-actin, J. Muscle Res. Cell Motil. 6 (1985) 129-151.
[81] E.K.L. Yeow, A.H.A. Clayton, Enumeration of Oligomerization States of Membrane Proteins in Living Cells by Homo-FRET Spectroscopy and Microscopy: Theory and Application, Biophys. J. 92 (2007) 3098-3104.
[82] J. Howard, A.A. Hyman, Dynamics and mechanics of the microtubule plus end, Nature 422 (2003) 753-758.

[83] M.P. Lillo, O. Canadas, R.E. Dale, A.U. Acuna, Location and properties of the taxol binding center in microtubules: A picosecond laser study with fluorescent taxoids, Biochemistry 41 (2002) 12436-12449.
[84] P. Brocca, L. Cantù, M. Cortia, E.D. Favero, A. Raudino, Collective phenomena in con ned micellar systems of gangliosides., Physica A 304 (2002) 177-190.
[85] C. Giacomelli, L.L. Men, R. Borsali, , Phosphorylcholine-Based pH-Responsive Diblock Copolymer Micelles as Drug Delivery Vehicles: Light Scattering, Electron Microscopy, and Fluorescence Experiments., Biomacromolecules 7 (2006) 817-828.
[86] M. Milnera, M. Štěpánek, I. Zusková, K. Procházka, Experimental Study of the Electrophoretic Mobility and Effective Electric Charge of Polystyrene-Block-Poly(Methacrylic Acid) Micelles in Aqueous Media, Inter. J. of Polym. Anal. Char. 12 (2007) 23-33.
[87] K. Schillén, A. Yekta, S. Ni, M.A. Winnik, Characterization by Fluorescence Energy Transfer of the Core of Polyisoprene-Poly(Methyl Methacrylate) Diblock Copolymer Micelles. Strong Segregation in Acetonitrile., Macromolecules 31 (1998) 210-212.
[88] G.M. Jones, C. Wofsy, C. Aurell, L.A. Sklar, Analysis of Vertical Fluorescence Resonance Energy Transfer from the Surface of a Small-Diameter Sphere., Biophys. J. 76 (1999) 517–527.
[89] G. Liu, C.K. Smith, N. Hu, J. Tao, Formation and Properties of Polystyrene-block-poly(2-hydroxyethyl methacrylate) Micelles., Macromolecules 29 (1996) 220-227.
[90] K. Procházka, B. Bednář, E. Mukhtar, P. Svoboda, J. Trněná, M. Almgren, Nonradiative Energy Transfer in Block Copolymer Micelles, J. Phys. Chem. 95 (1990) 4563-4568.
[91] K. Itaka, A. Harada, K. Nakamura, H. Kawaguchi, K. Kataoka, Evaluation by Fluorescence Resonance Energy Transfer of the Stability of Nonviral Gene Delivery Vectors under Physiological Conditions., Biomacromolecules 3 (2002) 841-845.
[92] A.K. Shaw, R. Sarkar, S.K. Pal, Direct observation of DNA condensation in a nano-cage by using a molecular ruler., Chem. Phys. Lett. 408 (2005) 366-370.
[93] J. Kim, M. Lee, Observation of multi-step conformation switching in b-amyloid peptide aggregation by fluorescence resonance energy transfer., Biochem. Biophys. Res. Com. 316 (2004) 393-397.
[94] R. Sarkar, A.K. Shaw, S.S. Narayanan, F. Dias, A. Monkman, S.K. Pal, Direct observation of protein folding in nanoenvironments using a molecular ruler., Biophys. Chem. 123 (2006) 40-48.
[95] Y. Taniguchi, T. Ikehara, K. N., H. Yamasaki, Y. Toyoshima, Dynamics of Light-Induced Conformational Changes of the Phoborhodopsin/Transducer Complex Formed in the n-Dodecyl b-D-Maltoside Micelle., Biochemistry 46 (2007) 5349-5357.
[96] S.L. Veatch, S.L. Keller, Seeing spots: Complex phase behavior in simple membranes., Biochim. Biophys. Acta 1746 (2005) 172-185.
[97] K. Simons, E. Ikonen, Functional rafts in cell membranes, Nature 387 (1997) 569-572.
[98] S.R. Mayor, M. Rao, Rafts: scale-dependent, active lipid organization at the cell surface., Traffic 5 (2004) 231-240.
[99] J.E. Shaw, R.F. Epand, R.M. Epand, Z. Li, R. Bittman, C.Y. Yip, Correlated Fluorescence-Atomic Force Microscopy of Membrane Domains: Structure of Fluorescence Probes Determines Lipid Localization., Biophys. J. 90 (2006) 2170-2178.
[100] A. Filippov, G. Orädd, G. Lindblom, Lipid Lateral Diffusion in Ordered and Disordered Phases in Raft Mixtures., Biophys. J. 86 (2004) 891-896.
[101] S. Pedersen, K. Jørgensen, T.R. Baekmark, O.G. Mouritsen, Indirect Evidence for Lipid-Domain Formation in the Transition Region of Phospholipid Bilayers by Two-Probe Fluorescence Energy Transfer., Biophys. J. 71 (1996) 554-560.
[102] I. Fedchina, P.-O. Westlund, Influence of molecular reorientation on electronic energy transfer betweena pair of mobile chromophores: The stochastic Liouville equataion combined with Brownian dynamic simulation techniques, Phys. Rev. E 50 (1994) 555-565.
[103] C. Leidy, W.F. Wolkers, K. Jørgensen, O.G. Mouritsen, J.H. Crowe, Lateral Organization and Domain Formation in a Two-Component Lipid Membrane System., Biophys. J. 80 (2001) 1819-1828.
[104] D. Marushchak, N. Gretskaya, I. Mikhalyov, L.B.-Å. Johansson, Self-aggregation - an intrinsic property of GM1 in lipid bilayers, Molec. Membrane Biol. 24 (2007) 102-112.

[105] R.F.M. de Almeida, L.M.S. Loura, A. Fedorov, M. Prieto, Lipid Rafts have Different Sizes Depending on Membrane Composition: A Time-resolved Fluorescence Resonance Energy Transfer Study., J. Mol. Biol. 346 (2005) 1109-1120.
[106] L.M.S. Loura, A. Fedorov, M. Prieto, Fluid–Fluid Membrane Microheterogeneity: A Fluorescence Resonance Energy Transfer Study., Biophys. J. 80 (2001) 776-788.
[107] K.B. Towles, A.C. Brown, S.P. Wrenn, N. Dan, Effect of Membrane Microheterogeneity and Domain Size on Fluorescence Resonance Energy Transfer., Biophys. J. 93 (2007) 655-667.
[108] A.C. Brown, K.B. Towles, S.P. Wrenn, Measuring Raft Size as a Function of Membrane Composition in PC-Based Systems: Part 1 - Binary Systems., Langmuir 23 (2007) 11180-11187.
[109] S. Mall, R. Broadbridge, R.P. Sharma, J.M. East, A.G. Lee, Self-Association of Model Transmembrane a-Helices Is Modulated by Lipid Structure., Biochemistry (2001) 12379-12386.
[110] E. Sparr, W.L. Ash, P.V. Nazarov, D.T.S. Rijkers, M.A. Hemminga, D.P. Tieleman, J.A. Killian, Self-association of Transmembrane a-Helices in Model Membranes., J. Biol. Chem. 280 (2005) 39324-39331.
[111] M. Bloom, E. Evans, O.G. Moritsen, Physical properties of the fluid lipid-bilayer component of cell membranes: a persepctive, Q. Rev. Biophys. 24 (1991) 293-297.
[112] H. Borochov-Neori, M. Montal, Rhodopsin-G-Protein Interactions Monitored by Resonance Energy Transfer., Biochemistry 28 (1989) 1711-1178.
[113] L.M.S. Loura, A. Coutinho, A. Silva, A. Fedorov, M. Prieto, Structural Effects of a Basic Peptide on the Organization of Dipalmitoylphosphatidylcholine/Dipalmitoylphosphatidylserine Membranes: A Fluorescent Resonance Energy Transfer Study., J. Phys. Chem. B 110 (2006) 8130-8141.
[114] S.-T. Bogen, G. de Korte-Kool, G. Lindblom, L.B.-Å. Johansson, Aggregation of an α- Helical Transmembrane Peptide in Lipid Phases, Studied by Time Resolved Fluorescence Spectroscopy, J. Phys. Chem. B 103 (1999) 8344-8352.
[115] H.E. Hasper, B. de Kruijff, E. Breukink, Assembly and Stability of Nisin-Lipid II Pores., Biochemistry 43 (2004) 11567-11575.
[116] Y. Tamba, M. Yamazaki, Single Giant Unilamellar Vesicle Method Reveals Effect of Antimicrobial Peptide Magainin 2 on Membrane Permeability., Biochemistry 44 (2005) 15823-15833.
[117] A. Miszta, R. Macháň, A. Benda, A.J. Ouellette, W.T. Hermens, M. Hof, Combination of ellipsometry, laser scanning microscopy and Z -scan fluorescence correlation spectroscopy elucidating interaction of cryptdin-4 with supported phospholipid bilayers., J. Pept. Sci. 14 (2008) 503-509.
[118] G. Viero, R. Cunaccia, G. Prévost, S. Werner, H. Monteil, D. Keller, O. Joubert, G. Menestrina, M.D. Serra, Homologous versus heterologous interactions in the bicomponent staphylococcal γ - haemolysin pore., Biochem. J. 394 (2006) 217-225.
[119] L.C. Silva, A., A. Fedorov, M. Prieto, Conformation and self-assembly of a nystatin nitrobenzoxadiazole derivative in lipid membranes., Biochim. Biophys. Acta 1617 (2003) 69-79.
[120] L.J. O'Neill, J.G. Miller, N.O. Petersen, Evidence for nystatin micelles in L-cell membranes from fluorescence photobleaching measurements of diffusion., Biochemistry 25 (1986) 177-181.
[121] C. Madeira, L.M.S. Loura, M.R. Aires-Barros, A. Fedorov, M. Prietoy, Characterization of DNA/Lipid Complexes by Fluorescence Resonance Energy Transfer., Biophys. J. 85 (2003) 3106-3119.
[122] K. Herrick-Davis, E. Grinde, J.E. Mazurkiewicz, Biochemical and Biophysical Characterization of Serotonin 5-HT2C Receptor Homodimers on the Plasma Membrane of Living Cells., Biochemistry 43 (2004) 13963-13971.
[123] J.R. Silvius, I.R. Nabi, Fluorescence-quenching and resonance energy transfer studies of lipid microdomains in model and biological membranes., Mol. Mem. Biol. 23 (2006) 5-16.
[124] A.K. Kenworthy, N. Petranova, M. Edidin, High-Resolution FRET Microscopy of Cholera Toxin B-Subunit and GPI-anchored Proteins in Cell Plasma Membranes., Mol. Biol. Cell 11 (2000) 1645-1655.
[125] P. Sharma, R. Varma, R.C. Sarasij, G.K. Ira, G. Krishnamoorthy, M. Rao, S. Mayor, Nanoscale Organization of Multiple GPI-Anchored Proteins in Living Cell Membranes., Cell 116 (2004) 577-589.
[126] P. Sengupta, D. Holowka, B. Baird, Fluorescence Resonance Energy Transfer between Lipid Probes Detects Nanoscopic Heterogeneity in the Plasma Membrane of Live Cells., Biophys. J. 92 (2007) 3564-3574.

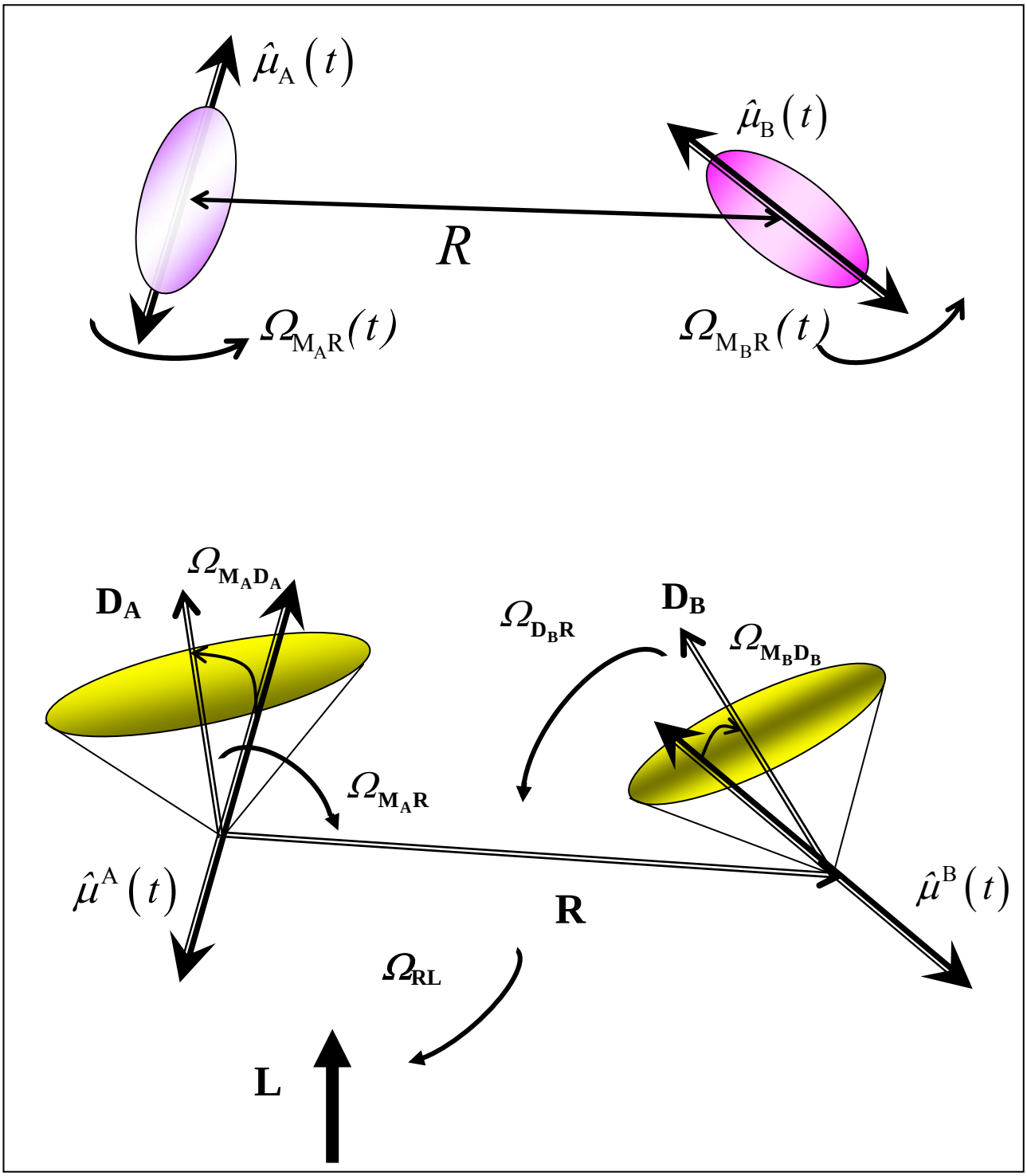

Fig. 1

Figure 1. The upper schematic shows two interacting chromophores A and B. These are either two donors, or one donor and one acceptor. A and B are thought to be covalently linked to a rigid macromolecule at a fixed distance (R), but they can undergo local reorienting motions in their binding sites. The local reorientations of the transition dipoles ($\hat{\mu}_A$ and $\hat{\mu}_B$) are described by the Eulerian angles ($\Omega_{M_jD_j}$, j = A or B) relative to the local coordinate systems $\mathbf{D}_A$ and $\mathbf{D}_B$. The different orientation transformations that relate the angular dependences (Ω_{lJ}) of the macromolecule, the A and B groups, as well as the energy transport to a laboratory coordinate system (**L**) are illustrated in the lower part of the figure. The Z-axis of the **R** frame connects the centres of mass of A and B.

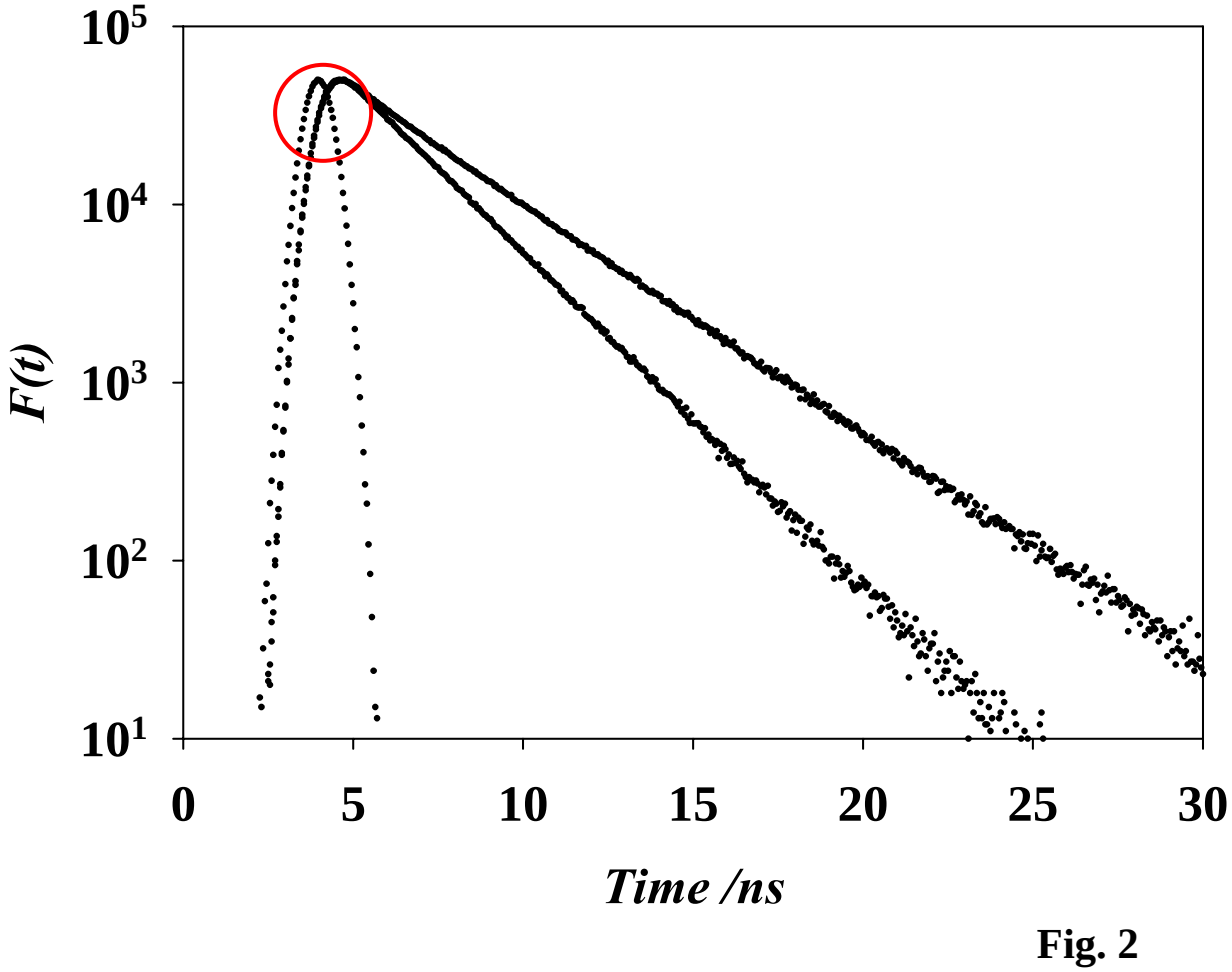

Fig. 2

Figure 2. Generated fluorescence relaxation data that mimic TCSPC experiments for DA-pairs of which the two groups are separated at a fixed distance $R = 0.8 \cdot R_0$. The lifetime of the donor $\tau_D = 10.0$ ns. The D and A groups are reorienting in an isotropic potential, *i.e.* the molecular order is isotropic. The photophysics' relaxation $\{F(t)\}$ of the D as predicted by the EFT (upper trace) and the FT. The ring indicates the time range where the FT agrees with the EFT

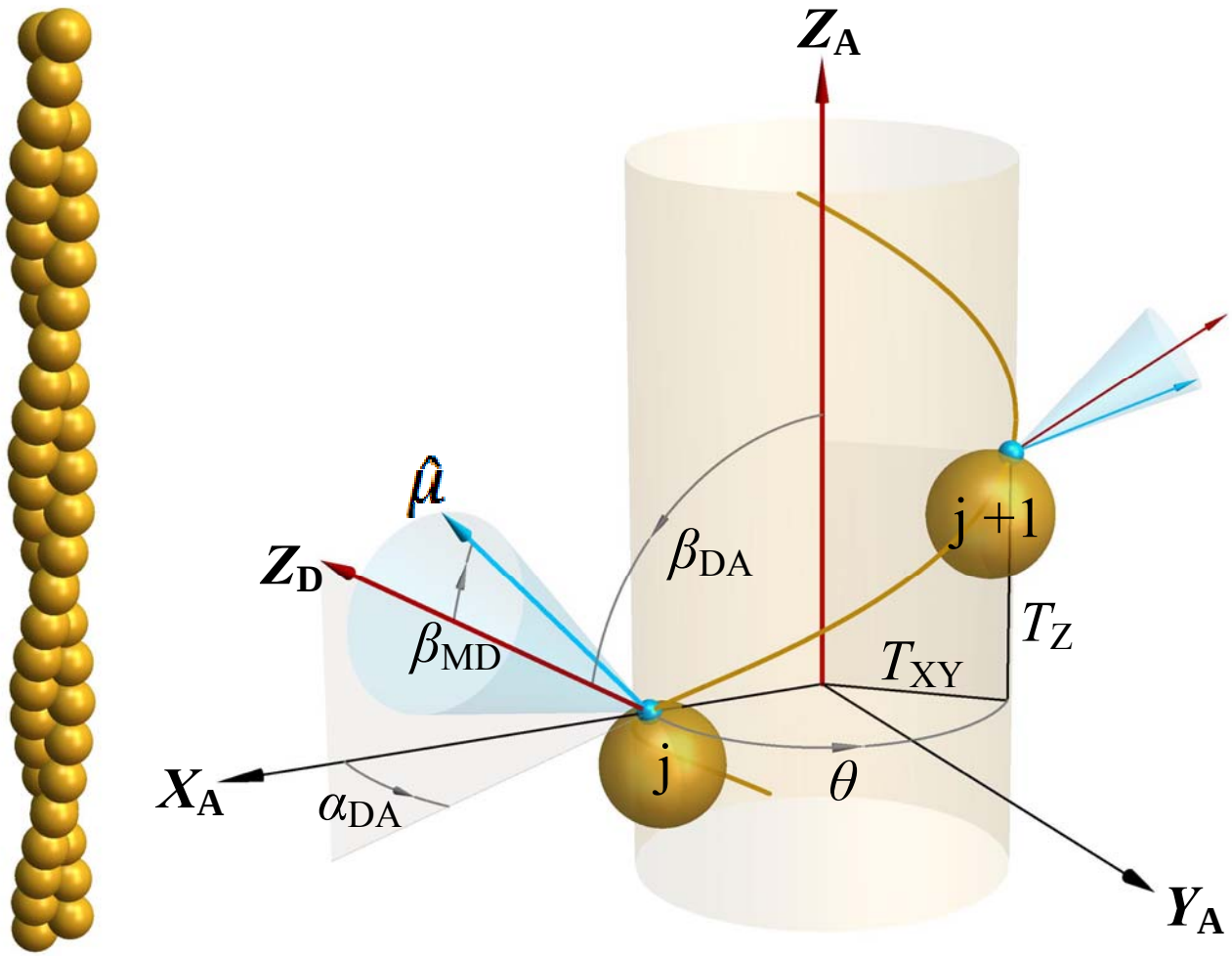

Fig. 3

Figure 3. Schematic showing the coordinate systems used to describe the protein position in regular structures forming helical, linear and ring-shaped aggregates. The Z_A axis coincides with the C_∞–axis of the aggregate and T_{xy} denotes the distance from this axis to the position of a fluorescent group. The translational and rotational transformations between nearest protein neighbours are θ and T_z, respectively. The fluorophore undergoes local reorienting motions about an effective symmetry axis Z_D that is transformed to the aggregate fixed frame by $\Omega_{DA} = (\alpha_{DA}, \beta_{DA})$. The electric transition dipole $\vec{\mu}$ is transformed to the D-frame by the angles $\Omega_{MD} = (\alpha_{MD}, \beta_{MD})$.

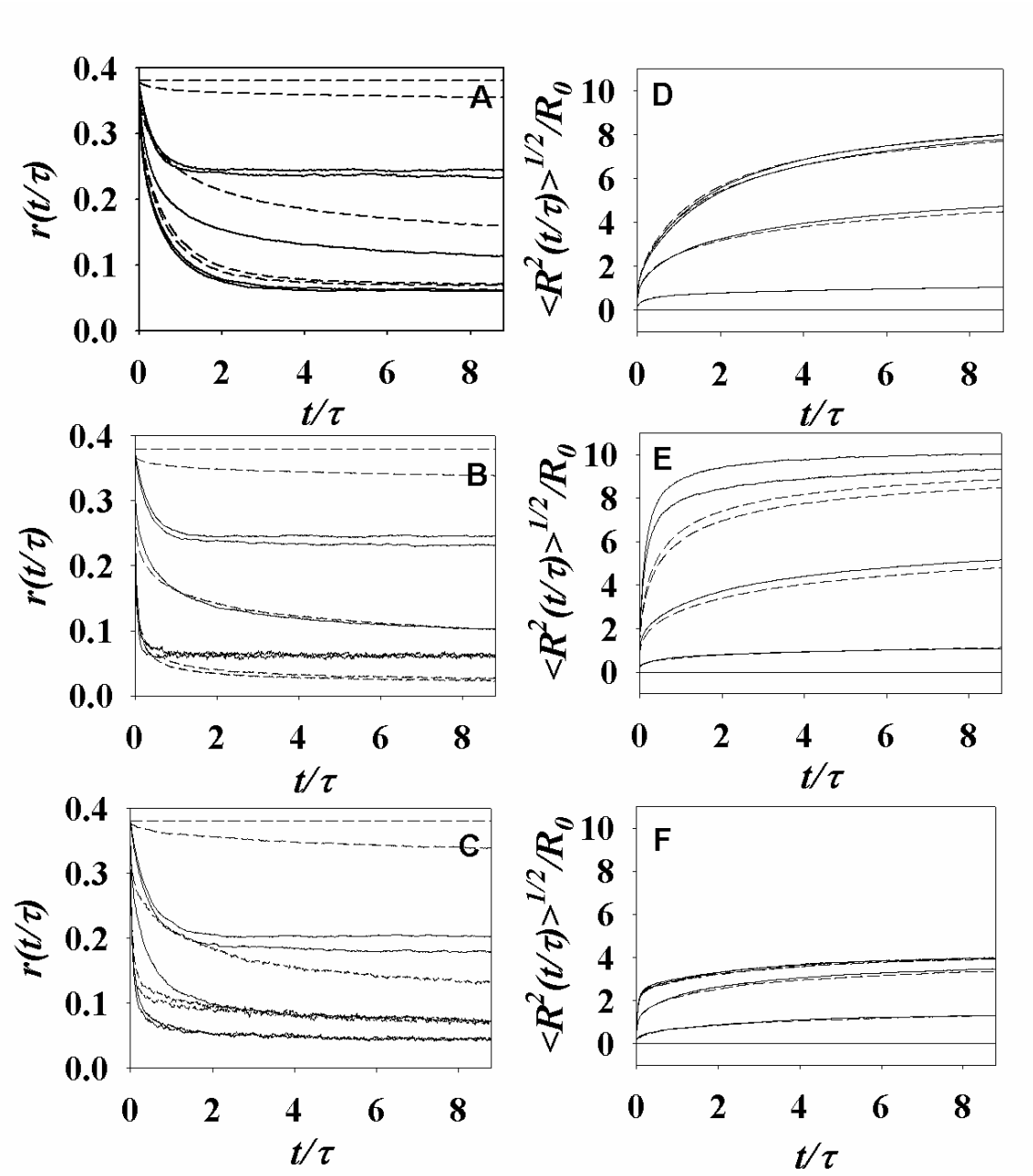

Fig. 4

Figure 4. The time-dependent anisotropy decay $\{r(t)\}$ and the normalised mean square displacement of the excitation $\{\langle R^2(t)\rangle^{1/2}/R_0\}$. The unit on the x-axis is reduced time, *i.e.* t/τ where τ is the fluorescence lifetime. The data refers to the following aggregate geometries: helical (**A**, **D**), linear (**B**, **E**) and circular (**C**, **F**). The dashed lines correspond to DDEM in the static limit (for local uniaxial anisotropic D-distribution), while the remaining *r(t)*-decays (solid lines) account for Brownian motions within the corresponding uniaxial Maier-Saupe potentials. The rotational correlation time is 0.86 in units of reduced time. In graphs **A**, **B** and **C** the residual anisotropy $\{r(t_\infty)\}$ decreases, while the mean square displacement (**D**, **E**, **F**) increases with increasing fraction of labelling. The labelling fractions (*f*) start by a very low value ($f \approx 10^{-4}$) and are increased to 5, 50, 95 and 100 %. The local order parameter $\langle D_{00}^{(2)}(\beta_{\mathrm{MD}})\rangle = 0.80$.

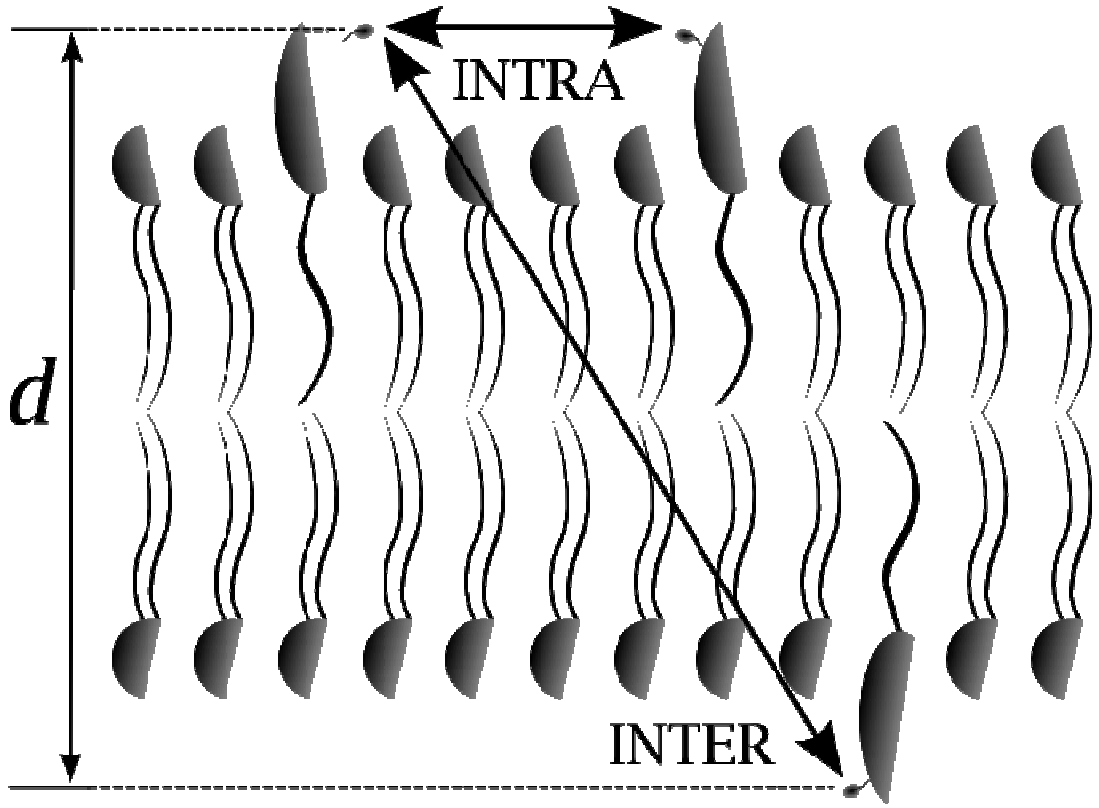

Fig. 5

Figure 5. Energy transfer/migration occurs either between fluorophore labels in one leaf of the lipid bilayer, *i.e.* an INTRA layer process, or between fluorophores located in different layers of bilayer, *i.e.* an INTER layer process. The energy transport is intra as well as inter between layers separated by the distance *d*.

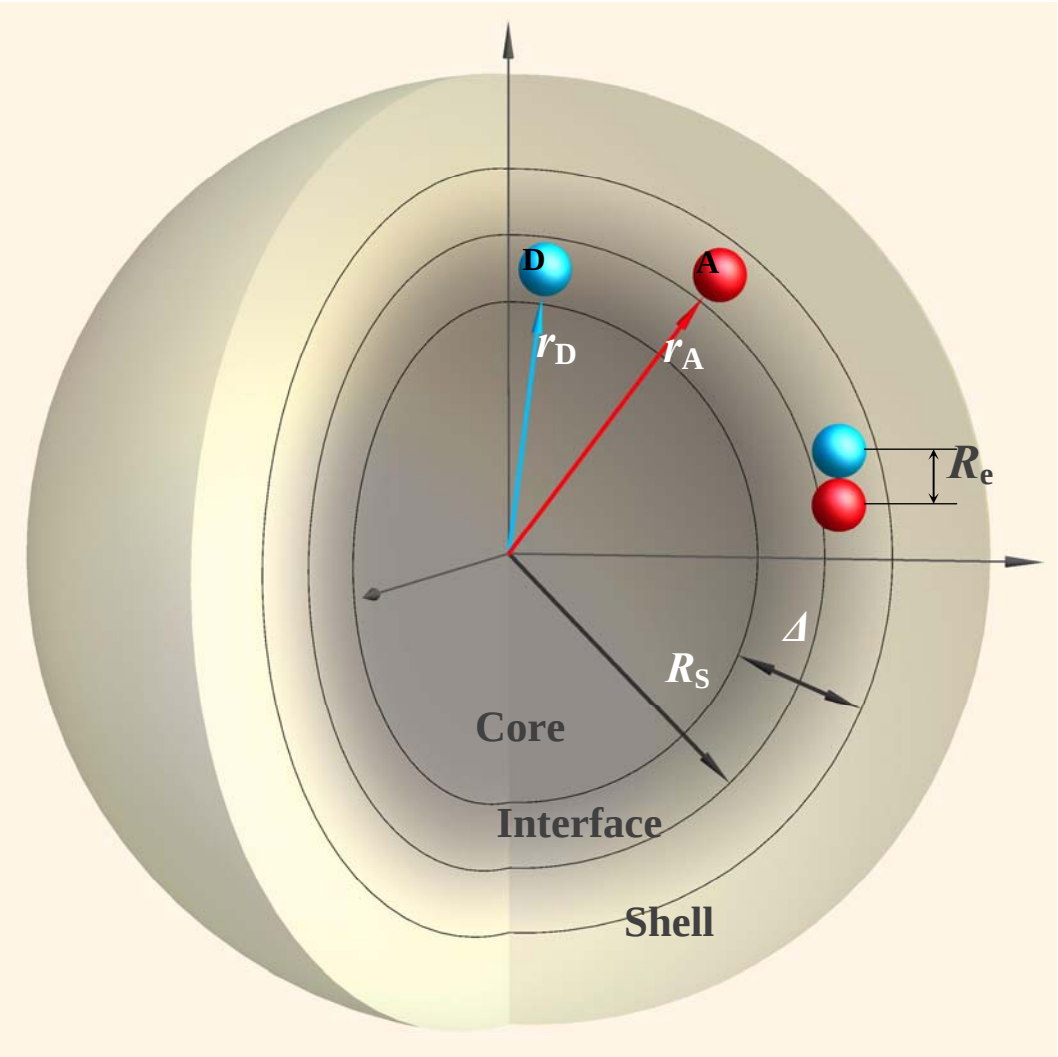

Fig. 6

Figure 6. A schematic of a spherical micelle, which indicates the core radius (R_s), the interface thickness (Δ), as well as the shell region. Donor and acceptor molecules are solubilised in the interface at the distances r_D or r_A, respectively. The encounter radius (R_e) refers to the shortest effective distance between the donor and acceptor molecules.